Title

Precise predictions for $\Lambda_b \to \Lambda_c$ semileptonic decays

Journal

Physical Review D, 99(5)

ISSN

2470-0010

Authors

Bernlochner, Florian U

Ligeti, Zoltan

Robinson, Dean J

et al.

Publication Date

2019-03-01

DOI

10.1103/physrevd.99.055008

Peer reviewed

Precise predictions for $\Lambda_b \to \Lambda_c$ semileptonic decays

Florian U. Bernlochner,[1] Zoltan Ligeti,[2] Dean J. Robinson,[2,3] and William L. Sutcliffe[1]

[1] *Karlsruher Institute of Technology, 76131 Karlsruhe, Germany*

[2] *Ernest Orlando Lawrence Berkeley National Laboratory, University of California, Berkeley, CA 94720, USA*

[3] *Santa Cruz Institute for Particle Physics and Department of Physics, University of California Santa Cruz, Santa Cruz, CA 95064, USA*

Abstract

We calculate the $\Lambda_b \to \Lambda_c \ell\nu$ form factors and decay rates for all possible $b \to c\ell\bar{\nu}$ four-Fermi interactions beyond the Standard Model, including nonzero charged lepton masses and terms up to order $\alpha_s\,\Lambda_{\rm QCD}/m_{c,b}$ and $\Lambda^2_{\rm QCD}/m_c^2$ in the heavy quark effective theory. At this order, we obtain model independent predictions for semileptonic $\Lambda_b \to \Lambda_c$ decays in terms of only two unknown sub-subleading Isgur-Wise functions, which can be determined from fitting LHCb and lattice QCD data. We thus obtain model independent results for $\Lambda_b \to \Lambda_c \ell\bar{\nu}$ decays, including predictions for the ratio $R(\Lambda_c) = \mathcal{B}(\Lambda_b \to \Lambda_c \tau\bar{\nu})/\mathcal{B}(\Lambda_b \to \Lambda_c \mu\bar{\nu})$ in the presence of new physics, that are more precise than prior results in the literature, and systematically improvable with better data on the decays with μ (or e) in the final state. We also explore tests of factorization in $\Lambda_b \to \Lambda_c \pi$ decays, and emphasize the importance of measuring at LHCb the double differential rate $d^2\Gamma(\Lambda_b \to \Lambda_c \ell\bar{\nu})/(dq^2\, d\cos\theta)$, in addition to the q^2 spectrum.

CONTENTS

I. INTRODUCTION

In a recent paper [1], it was shown that LHCb data for the semileptonic $\Lambda_b \to \Lambda_c \mu\nu$ decays [2] combined with lattice QCD calculations [3], provide sensitivity for the first time to sub-subleading $\mathcal{O}(\Lambda^2_{\rm QCD}/m_c^2)$ terms in the heavy quark effective theory (HQET) expansion [4, 5] of the $\Lambda_b \to \Lambda_c$ semileptonic decay form factors, independent of $|V_{cb}|$. The $\mathcal{O}(\Lambda^2_{\rm QCD}/m_c^2)$ corrections were found to have their expected characteristic size, suggesting that the expansion in $\Lambda_{\rm QCD}/m_c$ for baryon form factors is well-behaved up to $\Lambda^2_{\rm QCD}/m_c^2$ terms. The same framework also resulted in a new standard model (SM) prediction for the ratio

$$R(\Lambda_c) = \frac{\Gamma(\Lambda_b \to \Lambda_c \tau \bar{\nu})}{\Gamma(\Lambda_b \to \Lambda_c \mu \bar{\nu})} = 0.324 \pm 0.004\,, \tag{1}$$

which is significantly more precise than prior results [3, 6–11].

The ratio in Eq. (1) is of particular interest in light of the persistent hints of deviations from the SM, in the ratios

$$R(D^{(*)}) = \frac{\Gamma(B \to D^{(*)} \tau \bar{\nu})}{\Gamma(B \to D^{(*)} l \bar{\nu})}\,, \qquad l = \mu, e\,, \tag{2}$$

at approximately the 4σ level, once the measurements for the D and D^* final states are combined [12]. The $\Lambda_b \to \Lambda_c \mu \bar{\nu}$ decays involve the same underlying $b \to c\tau\nu$ new physics (NP) operators as $B \to D^{(*)} \tau \bar{\nu}$, but the HQET expansion for the ground-state baryon form factors is simpler than for mesons. The "brown muck" surrounding the heavy quark is in a spin and isospin zero ground state. A consequence of this is a simpler expansion of the form factors, in which the $\mathcal{O}(\Lambda_{\rm QCD}/m_{c,b}\,,\ \alpha_s\,\Lambda_{\rm QCD}/m_{c,b})$ subleading contributions are determined by the leading order Isgur-Wise function, reducing the number of free parameters in the form factor fits, and thereby providing sensitivity to $\mathcal{O}(\Lambda^2_{\rm QCD}/m_c^2)$ terms.

The spread in the uncertainties quoted for theoretical predictions for $R(D^*)$ in the SM are largely due to different estimates of $\mathcal{O}(\Lambda^2_{\rm QCD}/m_c^2)$ effects [13–15]. The very same hadronic matrix elements are also crucial to resolve tensions between inclusive and exclusive determinations of $|V_{cb}|$ [13–21]. The abundant sample of Λ_b baryons produced at the LHC may therefore provide a complementary and theoretically cleaner laboratory to study the behavior of the heavy quark expansion, identify possible NP effects, and extract $|V_{cb}|$.

In this paper, we expand and generalize the study of Ref. [1] beyond the SM, to include all $b \to c\tau\bar{\nu}$ four-Fermi operators, including those containing right-handed (sterile) neutrinos.

We compute the relevant form factors including $\mathcal{O}(\Lambda_{\rm QCD}^2/m_c^2)$ terms, and compare the fit results of Ref. [1] to the lattice QCD determinations of not only the three vector and three axial vector SM form factors, but also the four NP tensor current form factors. We further emphasize the importance of measuring at LHCb the double differential rate $d^2\Gamma(\Lambda_b \to \Lambda_c \ell \bar\nu)/(dq^2\, d\cos\theta)$ in addition to the q^2 spectrum, and also explore tests of factorization in $\Lambda_b \to \Lambda_c \pi$ decay.

II. HQET EXPANSION OF THE FORM FACTORS

A. Form factor definitions

We are interested in the $\Lambda_b \to \Lambda_c$ matrix elements of operators with all possible Dirac structures, for which we choose the basis

$$\begin{aligned} &O_V = \bar c\,\gamma_\mu\, b\,, && O_A = \bar c\,\gamma_\mu\gamma_5\, b\,, \\ &O_S = \bar c\, b\,, && O_P = \bar c\,\gamma_5\, b\,, && O_T = \bar c\,\sigma_{\mu\nu}\, b\,, \end{aligned} \tag{3}$$

with $\sigma_{\mu\nu} = (i/2)\,[\gamma_\mu, \gamma_\nu]$. As done in Refs. [22–25] for excited charm mesons, we use the conventions $\mathrm{Tr}[\gamma^\mu\gamma^\nu\gamma^\sigma\gamma^\rho\gamma^5] = -4i\epsilon^{\mu\nu\rho\sigma}$, so that $\sigma^{\mu\nu}\gamma^5 \equiv +(i/2)\epsilon^{\mu\nu\rho\sigma}\sigma_{\rho\sigma}$. (This is the opposite of the common convention in the $\overline{B} \to D^{(*)}\ell\bar\nu$ literature, which typically chooses $\mathrm{Tr}[\gamma^\mu\gamma^\nu\gamma^\sigma\gamma^\rho\gamma^5] = +4i\epsilon^{\mu\nu\rho\sigma}$, so that $\sigma^{\mu\nu}\gamma^5 \equiv -(i/2)\epsilon^{\mu\nu\rho\sigma}\sigma_{\rho\sigma}$.)

The semileptonic $\Lambda_b \to \Lambda_c \ell\bar\nu$ form factors in HQET are conventionally defined for the SM currents as [26–28]

$$\begin{aligned} \langle \Lambda_c(p',s')|\bar c\gamma_\nu b|\Lambda_b(p,s)\rangle &= \bar u(p',s')\big[f_1\gamma_\mu + f_2 v_\mu + f_3 v'_\mu\big]u(p,s)\,, \\ \langle \Lambda_c(p',s')|\bar c\gamma_\nu\gamma_5 b|\Lambda_b(p,s)\rangle &= \bar u(p',s')\big[g_1\gamma_\mu + g_2 v_\mu + g_3 v'_\mu\big]\gamma_5\, u(p,s)\,, \end{aligned} \tag{4}$$

where $p = m_{\Lambda_b} v$, $p' = m_{\Lambda_c} v'$, and the f_i and g_i are functions of $w = v\cdot v' = (m_{\Lambda_b}^2 + m_{\Lambda_c}^2 - q^2)/(2m_{\Lambda_b} m_{\Lambda_c})$. The spinors are normalized to $\bar u(p,s)u(p,s) = 2m$. We further define the NP form factors,

$$\begin{aligned} \langle \Lambda_c(p',s')|\bar c\, b|\Lambda_b(p,s)\rangle &= h_S\,\bar u(p',s')\,u(p,s)\,, \\ \langle \Lambda_c(p',s')|\bar c\gamma_5 b|\Lambda_b(p,s)\rangle &= h_P\,\bar u(p',s')\,\gamma_5\,u(p,s)\,, \\ \langle \Lambda_c(p',s')|\bar c\,\sigma_{\mu\nu}\, b|\Lambda_b(p,s)\rangle &= \bar u(p',s')\big[h_1\,\sigma_{\mu\nu} + i\,h_2(v_\mu\gamma_\nu - v_\nu\gamma_\mu) + i\,h_3(v'_\mu\gamma_\nu - v'_\nu\gamma_\mu) \\ &\qquad + i\,h_4(v_\mu v'_\nu - v_\nu v'_\mu)\big]u(p,s)\,. \end{aligned} \tag{5}$$

In the definition of the NP tensor current, the conventions are chosen to simplify the α_s corrections when expressed in terms of the standard coefficient functions.

In full QCD, the form factors of the SM currents were instead traditionally defined as [27],

$$\begin{aligned}\langle\Lambda_c(p',s')|\bar{c}\gamma_\mu b|\Lambda_b(p,s)\rangle &= \bar{u}(p',s')\big[F_1\,\gamma_\mu - iF_2\,\sigma_{\mu\nu}\,q^\nu + F_3\,q_\mu\big]u(p,s)\,,\\ \langle\Lambda_c(p',s')|\bar{c}\gamma_\mu\gamma_5 b|\Lambda_b(p,s)\rangle &= \bar{u}(p',s')\big[G_1\,\gamma_\mu - iG_2\,\sigma_{\mu\nu}\,q^\nu + G_3\,q_\mu\big]\gamma_5\,u(p,s)\,.\end{aligned} \tag{6}$$

Our notation for the form factors follows Ref. [28]; the notation of Ref. [27] corresponds to an exchange of upper and lowercase symbols, $F_i \leftrightarrow f_i$ and $G_i \leftrightarrow g_i$, in Eqs. (4) and (6). The relations between the form factors in Eqs. (4) and (6) are given in the Appendix A.

B. Form factors in HQET

The ground state baryons are singlets of heavy quark spin symmetry, because the light degrees of freedom, the "brown muck", are in the spin-0 state. Hence, the baryon masses can be written as

$$m_{\Lambda_Q} = m_Q + \bar{\Lambda}_\Lambda - \frac{\lambda_1^\Lambda}{2m_Q} + \dots\,, \qquad Q = b, c\,, \tag{7}$$

where the ellipsis denote terms suppressed by more powers of $\Lambda_{\rm QCD}/m_Q$. The parameter $\bar{\Lambda}_\Lambda$ is the energy of the light degrees of freedom in the $m_Q \to \infty$ limit. The λ_1^Λ parameter is related to the heavy quark kinetic energy in the Λ baryon. We use $m_{\Lambda_b} = 5.620\,\text{GeV}$, $m_{\Lambda_c} = 2.286\,\text{GeV}$ [29], and employ the $1S$ short distance mass scheme [30–32] to eliminate the leading renormalon ambiguities in the definition of the quark masses and $\bar{\Lambda}_\Lambda$. Details of the $1S$ scheme treatment can be found in Ref. [13]. In particular, we treat $m_b^{1S} = (4.71 \pm 0.05)\,\text{GeV}$ and $\delta m_{bc} = m_b - m_c = (3.40 \pm 0.02)\,\text{GeV}$ as independent parameters [33]. (The latter is well constrained by $B \to X_c\ell\bar{\nu}$ spectra [34, 35].) We match HQET onto QCD at scale $\mu = \sqrt{m_b m_c}$, so that $\alpha_s \simeq 0.26$. For example, using Eq. (7) for both Λ_b and Λ_c to eliminate λ_1^Λ, at $\mathcal{O}(\alpha_s)$ we obtain $\bar{\Lambda}_\Lambda = (0.81 \pm 0.05)\,\text{GeV}$ and $\lambda_1^\Lambda = -(0.24 \pm 0.08)\,\text{GeV}^2$. (Similar HQET-based discussions can be found for other decay modes, $B \to D^{(*)}\ell\bar{\nu}$ [13], $B \to D^{**}\ell\bar{\nu}$ [22–25], and $\Lambda_b \to \Lambda_c^*\ell\bar{\nu}$ [36, 37].)

Making the transition to HQET [4, 5], at leading order in $\Lambda_{\rm QCD}/m_{c,b}$,

$$\langle\Lambda_c(v',s')|\bar{c}\,\Gamma b\,|\Lambda_b(v,s)\rangle = \zeta(w)\,\bar{u}(v',s')\,\Gamma\,u(v,s)\,, \tag{8}$$

where $u(v,s)$ satisfies $\not{v}\, u(v,s) = u(v,s)$ and $\zeta(w)$ is the Isgur-Wise function for ground state baryons [26], satisfying $\zeta(1) = 1$. At leading order, one finds

$$\begin{aligned} &f_1(w) = g_1(w) = h_S(w) = h_P(w) = h_1(w) = \zeta(w)\,, \\ &f_2(w) = f_3(w) = g_2(w) = g_3(w) = h_2(w) = h_3(w) = h_4(w) = 0\,. \end{aligned} \tag{9}$$

At order $\Lambda_{\rm QCD}/m_{c,b}$ a remarkable simplification occurs compared to meson decays. The $\mathcal{O}(\Lambda_{\rm QCD}/m_{c,b})$ corrections from the matching of the $\bar{c}\,\Gamma b$ heavy quark current onto HQET [38–40] can be expressed in terms of $\bar{\Lambda}_\Lambda$ and the leading order Isgur-Wise function $\zeta(w)$ [41]. In addition, for $\Lambda_b \to \Lambda_c$ transitions, i.e., between the ground state baryons, there are no $\mathcal{O}(\Lambda_{\rm QCD}/m_{c,b})$ contributions from the chromomagnetic operator. The kinetic energy operator in the $\mathcal{O}(\Lambda_{\rm QCD}/m_{c,b})$ HQET Lagrangian gives rise to a heavy quark spin symmetry conserving subleading term, parametrized by $\zeta_{\rm ke}(w)$, which can be absorbed into the leading order Isgur-Wise function by redefining ζ via

$$\zeta(w) + (\varepsilon_c + \varepsilon_b)\,\zeta_{\rm ke}(w) \to \zeta(w)\,, \tag{10}$$

where $\varepsilon_{c,b} = \bar{\Lambda}_\Lambda/(2\,m_{c,b})$. Luke's theorem [42] implies $\zeta_{\rm ke}(1) = 0$, so the normalization $\zeta(1) = 1$ is preserved. Thus, no additional unknown functions beyond $\zeta(w)$ are needed to parametrize the $\mathcal{O}(\Lambda_{\rm QCD}/m_{c,b})$ corrections. Perturbative corrections to the heavy quark currents can be computed by matching QCD onto HQET [38–40], and introduce no new hadronic parameters. The same also holds for the order $\alpha_s\,\Lambda_{\rm QCD}/m_{c,b}$ corrections [43, 44].

The $\mathcal{O}(\Lambda^2_{\rm QCD}/m^2_{c,b})$ corrections are parametrized by six linear combinations of sub-subleading Isgur-Wise functions, $b_{1,\ldots,6}$ [27], which are functions of w. Only two of these, $b_{1,2}(w)$, occur at $\mathcal{O}(\Lambda^2_{\rm QCD}/m^2_c)$. The redefinition in Eq. (10) introduces additional $\epsilon_c^2\,\zeta_{\rm ke}(w)$ terms, which can be reabsorbed into $b_{1,2}(w)$. We may then define

$$\big\{\hat{f}_i(w)\,,\ \hat{g}_i(w)\,,\ \hat{h}_i(w),\ \hat{b}_i(w)\big\} = \big\{f_i(w)\,,\ g_i(w)\,,\ h_i(w)\,,\ b_i(w)\big\}/\zeta(w)\,. \tag{11}$$

Thus, including α_s, $\Lambda_{\rm QCD}/m_{c,b}$, $\alpha_s\,\Lambda_{\rm QCD}/m_{c,b}$, and $\Lambda^2_{\rm QCD}/m^2_c$ corrections, the SM form factors are [1]

$$\begin{aligned} \hat{f}_1 &= 1 + \hat{\alpha}_s C_{V_1} + \varepsilon_c + \varepsilon_b + \hat{\alpha}_s\Big[C_{V_1} + 2(w-1)C'_{V_1}\Big](\varepsilon_c + \varepsilon_b) + \frac{\hat{b}_1 - \hat{b}_2}{4m_c^2} + \ldots\,, \\ \hat{f}_2 &= \hat{\alpha}_s C_{V_2} - \frac{2\,\varepsilon_c}{w+1} + \hat{\alpha}_s\bigg[C_{V_2}\frac{3w-1}{w+1}\varepsilon_b - \big[2C_{V_1} - (w-1)C_{V_2} + 2C_{V_3}\big]\frac{\varepsilon_c}{w+1} \\ &\quad + 2(w-1)C'_{V_2}(\varepsilon_c + \varepsilon_b)\bigg] + \frac{\hat{b}_2}{4m_c^2} + \ldots\,, \end{aligned}$$

$$
\begin{aligned}
\hat{f}_3 &= \hat{\alpha}_s C_{V_3} - \frac{2\,\varepsilon_b}{w+1} + \hat{\alpha}_s \bigg[C_{V_3} \frac{3w-1}{w+1} \varepsilon_c - \big[2C_{V_1} + 2C_{V_2} - (w-1)C_{V_3}\big] \frac{\varepsilon_b}{w+1} \\
&\quad + 2(w-1) C'_{V_3} (\varepsilon_c + \varepsilon_b) \bigg] + \dots \,, \\
\hat{g}_1 &= 1 + \hat{\alpha}_s C_{A_1} + (\varepsilon_c + \varepsilon_b) \frac{w-1}{w+1} + \hat{\alpha}_s \bigg[C_{A_1} \frac{w-1}{w+1} + 2(w-1) C'_{A_1} \bigg] (\varepsilon_c + \varepsilon_b) + \frac{\hat{b}_1}{4m_c^2} + \dots \,, \\
\hat{g}_2 &= \hat{\alpha}_s C_{A_2} - \frac{2\,\varepsilon_c}{w+1} + \hat{\alpha}_s \bigg[C_{A_2} \frac{3w+1}{w+1} \varepsilon_b - \big[2C_{A_1} - (w+1)C_{A_2} + 2C_{A_3}\big] \frac{\varepsilon_c}{w+1} \\
&\quad + 2(w-1) C'_{A_2} (\varepsilon_c + \varepsilon_b) \bigg] + \frac{\hat{b}_2}{4m_c^2} + \dots \,, \\
\hat{g}_3 &= \hat{\alpha}_s C_{A_3} + \frac{2\,\varepsilon_b}{w+1} + \hat{\alpha}_s \bigg[C_{A_3} \frac{3w+1}{w+1} \varepsilon_c + \big[2C_{A_1} - 2C_{A_2} + (w+1)C_{A_3}\big] \frac{\varepsilon_b}{w+1} \\
&\quad + 2(w-1) C'_{A_3} (\varepsilon_c + \varepsilon_b) \bigg] + \dots \,,
\end{aligned}
\tag{12}
$$

where the C_{Γ_i} are functions of w, and $\hat{\alpha}_s = \alpha_s/\pi$. (We use the notation of Ref. [28]; explicit expressions for C_{Γ_i} are in Ref. [13].) In Eq. (12), primes denote $\partial/\partial w$ and the ellipses denote $\mathcal{O}(\varepsilon_c\varepsilon_b,\, \varepsilon_b^2,\, \varepsilon_c^3)$ and higher order terms in $\Lambda_{\rm QCD}/m_Q$ and/or α_s. Equation (12) agrees with Eq. (4.75) in Ref. [44] (where a redefinition different from Eq. (10) was used).

For the expansions of the form factors parametrizing the BSM currents, we obtain,

$$
\begin{aligned}
\hat{h}_S &= 1 + \hat{\alpha}_s\, C_S + (\varepsilon_c + \varepsilon_b) \frac{w-1}{w+1} + \hat{\alpha}_s \bigg[C_S \frac{w-1}{w+1} + 2(w-1) C'_S \bigg] (\varepsilon_c + \varepsilon_b) + \frac{\hat{b}_1}{4m_c^2} + \dots \,, \\
\hat{h}_P &= 1 + \hat{\alpha}_s\, C_P + \varepsilon_c + \varepsilon_b + \hat{\alpha}_s \bigg[C_P + 2(w-1) C'_P \bigg] (\varepsilon_c + \varepsilon_b) + \frac{\hat{b}_1 - \hat{b}_2}{4m_c^2} + \dots \,, \\
\hat{h}_1 &= 1 + \hat{\alpha}_s\, C_{T_1} + (\varepsilon_c + \varepsilon_b) \frac{w-1}{w+1} + \hat{\alpha}_s \bigg[C_{T_1} \frac{w-1}{w+1} + 2(w-1) C'_{T_1} \bigg] (\varepsilon_c + \varepsilon_b) + \frac{\hat{b}_1}{4m_c^2} + \dots \,, \\
\hat{h}_2 &= \hat{\alpha}_s\, C_{T_2} - \frac{2\,\varepsilon_c}{w+1} + \hat{\alpha}_s \bigg[C_{T_2} \frac{3w+1}{w+1} \varepsilon_b - \big[2C_{T_1} - (w+1)C_{T_2} + 2C_{T_3}\big] \frac{\varepsilon_c}{w+1} \\
&\quad + 2(w-1) C'_{T_2} (\varepsilon_c + \varepsilon_b) \bigg] + \frac{\hat{b}_2}{4m_c^2} + \dots \,, \\
\hat{h}_3 &= \hat{\alpha}_s\, C_{T_3} + \frac{2\,\varepsilon_b}{w+1} + \hat{\alpha}_s \bigg[C_{T_3} \frac{3w+1}{w+1} \varepsilon_c + \big[2C_{T_1} - 2C_{T_2} + (w+1)C_{T_3}\big] \frac{\varepsilon_b}{w+1} \\
&\quad + 2(w-1) C'_{T_3} (\varepsilon_c + \varepsilon_b) \bigg] + \dots \,, \\
\hat{h}_4 &= \hat{\alpha}_s \frac{2}{w+1} \big(C_{T_3} \varepsilon_c - C_{T_2} \varepsilon_b \big) + \dots \,.
\end{aligned}
\tag{13}
$$

Similar to f_3 and g_3, neither of the h_3 and h_4 form factors receive $\Lambda_{\rm QCD}^2/m_c^2$ corrections. The structure of $h_{1,2,3}$ is similar to $g_{1,2,3}$, while h_4 is non-zero only at $\mathcal{O}(\alpha_s\, \Lambda_{\rm QCD}/m_{c,b})$.

C. Differential decay rates and forward-backward asymmetry

In Appendix B, we collect explicit expressions for the $\Lambda_b \to \Lambda_c \ell \nu$ amplitudes for all NP operators, including contributions from massless right-handed sterile neutrinos [45, 46]. Including the charged lepton mass dependence, and defining θ as the angle between the lepton and the Λ_c momentum in the dilepton rest frame,[1] the SM double differential decay rate is

$$\frac{d^2\Gamma}{dw\, d\cos\theta} = \frac{G_F^2\, m_{\Lambda_b}^5 |V_{cb}|^2}{48\,\pi^3}\, \frac{(\hat{q}^2-\rho_\ell)^2}{\hat{q}^4}\, r_\Lambda^3\, \sqrt{w^2-1}\, \Bigg[\left(1+\frac{\rho_\ell}{2\hat{q}^2}\right)\Big(\mathcal{H}_+ + 2\hat{q}^2\mathcal{H}_1\Big) + \frac{3\rho_\ell}{2\hat{q}^2}\,\mathcal{H}_0 - 3\sqrt{w^2-1}\left(2 f_1\, g_1\, \hat{q}^2 - \frac{\rho_\ell}{\hat{q}^2}\,\mathcal{H}_{+0}\right)\cos\theta + \left(1-\frac{\rho_\ell}{\hat{q}^2}\right)\Big(\hat{q}^2\,\mathcal{H}_1 - \mathcal{H}_+\Big)\frac{3\cos^2\theta-1}{2}\Bigg], \tag{14}$$

where $\rho_\ell = m_\ell^2/m_{\Lambda_b}^2$, $r_\Lambda = m_{\Lambda_c}/m_{\Lambda_b}$, $\hat{q}^2 \equiv q^2/m_{\Lambda_b}^2 = 1 - 2 r_\Lambda w + r_\Lambda^2$,

$$\begin{aligned} \mathcal{H}_1 &= (w-1) f_1^2 + (w+1) g_1^2\,, & \mathcal{H}_+ &= (w-1)\mathcal{F}_+^2 + (w+1)\mathcal{G}_+^2\,, \\ \mathcal{H}_0 &= (w+1)\mathcal{F}_0^2 + (w-1)\mathcal{G}_0^2\,, & \mathcal{H}_{+0} &= \mathcal{F}_+\mathcal{F}_0 + \mathcal{G}_+\mathcal{G}_0\,, \end{aligned} \tag{15}$$

and

$$\begin{aligned} \mathcal{F}_+ &= (1+r_\Lambda) f_1 + (w+1)(r_\Lambda\, f_2 + f_3)\,, \\ \mathcal{G}_+ &= (1-r_\Lambda) g_1 - (w-1)(r_\Lambda\, g_2 + g_3)\,, \\ \mathcal{F}_0 &= (1-r_\Lambda) f_1 - (r_\Lambda w - 1) f_2 + (w - r_\Lambda) f_3\,, \\ \mathcal{G}_0 &= (1+r_\Lambda) g_1 + (r_\Lambda w - 1) g_2 - (w - r_\Lambda) g_3\,. \end{aligned} \tag{16}$$

The double differential rate in Eq. (14) can be at most a degree-two polynomial in $\cos\theta$, and it was written in Eq. (14) in the Legendre polynomial basis, so that only the zeroth order term in the first line contributes to the $d\Gamma/dq^2$, after integration over $d\cos\theta$.

The single differential rate in the SM is correspondingly

$$\frac{d\Gamma}{dw} = \frac{G_F^2\, m_{\Lambda_b}^5 |V_{cb}|^2}{24\,\pi^3}\, \frac{(\hat{q}^2-\rho_\ell)^2}{\hat{q}^4}\, r_\Lambda^3\, \sqrt{w^2-1}\, \Bigg[\left(1+\frac{\rho_\ell}{2\hat{q}^2}\right)\Big(\mathcal{H}_+ + 2\hat{q}^2\mathcal{H}_1\Big) + \frac{3\rho_\ell}{2\hat{q}^2}\,\mathcal{H}_0\Bigg], \tag{17}$$

and the forward-backward asymmetry is given by

$$\begin{aligned} \frac{dA_{\rm FB}}{dw} &= \left[\int_0^1 - \int_{-1}^0\right] \frac{d^2\Gamma}{dw\, d\cos\theta}\, d\cos\theta \\ &= -\frac{G_F^2\, m_{\Lambda_b}^5 |V_{cb}|^2}{16\,\pi^3}\, \frac{(\hat{q}^2-\rho_\ell)^2}{\hat{q}^4}\, r_\Lambda^3\, (w^2-1)\left(2 f_1\, g_1\, \hat{q}^2 - \frac{\rho_\ell}{\hat{q}^2}\,\mathcal{H}_{+0}\right). \end{aligned} \tag{18}$$

[1] This angle is not measurable in the τ channel by present experiments, because neither the Λ_b nor τ momentum can be precisely reconstructed. In principle, if the Λ_b momentum was known and the $\tau \to 3\pi\nu$ decay mode was used to reconstruct the τ vertex, then θ could be reconstructed.

Our result in Eq. (17) agrees with those in Refs. [3, 47]. Including all possible NP current operators and a nonzero charged lepton mass, our result for $d\Gamma/dw$ as derived from Appendix B agrees with the result for SM neutrinos in Eq. (2.51) of Ref. [48]. We see from Eqs. (14) or (18) that the θ distribution in the light lepton modes gives sensitivity to the product $f_1\, g_1$, which is not present in $d\Gamma/dw$. The quadratic term in $\cos\theta$ in the angular distribution provides sensitivity to the combination $\hat{q}^2\mathcal{H}_1 - \mathcal{H}_+$. Thus, just like in the case of $b \to s\ell^+\ell^-$ [49], measuring the dependencies on all three polynomials of $\cos\theta$, gives information on the form factors beyond measuring only $d\Gamma/dq^2$ and $dA_{\rm FB}/dq^2$.

To gain more information than obtainable from Eq. (14), the distribution of the Λ_c decay products would have to be studied. Such an analysis would be simplest for two-body decays, such as $\Lambda_c \to \Lambda(p\pi^-)\pi^+$ [7]. This channel loses an order of magnitude in statistics compared to the commonly used $\Lambda_c \to pK\pi$ reconstruction, however, a model independent description of this three-body decay amplitude is not currently available. With much higher statistics and using $\Lambda_c \to \Lambda\pi^+$, the measurement of all $\Lambda_b \to \Lambda_c$ form factors would be similar to that for $\Lambda_c \to \Lambda e\nu$ [50–52], requiring measuring distributions in three angles (as for $B \to (D^* \to D\pi)l\bar{\nu}$).

If NP only modifies the (axial)vector interactions (see e.g. Refs. [7, 9, 53] for other cases), which may be the most plausible scenario, then Eqs. (14) – (18) are simply modified via the replacements

$$f_i \to f_i(1 + g_L + g_R)\,, \qquad g_i \to g_i(1 + g_L - g_R)\,, \tag{19}$$

and, in particular,

$$\frac{dA_{\rm FB}}{dw} \to \frac{dA_{\rm FB}}{dw}\left[(1+g_L)^2 - g_R)^2\right]. \tag{20}$$

In the $m_l = 0$ limit, i.e., in the $\Lambda_c\mu\nu$ and $\Lambda_c e\nu$ modes, the forward-backward asymmetry only receives further contributions from tensor–(pseudo)scalar interference, even in the presence of arbitrary NP. The relation in Eq. (20) is then valid in the light lepton modes, as long as NP does not simultaneously generate (pseudo)scalar and tensor operators.

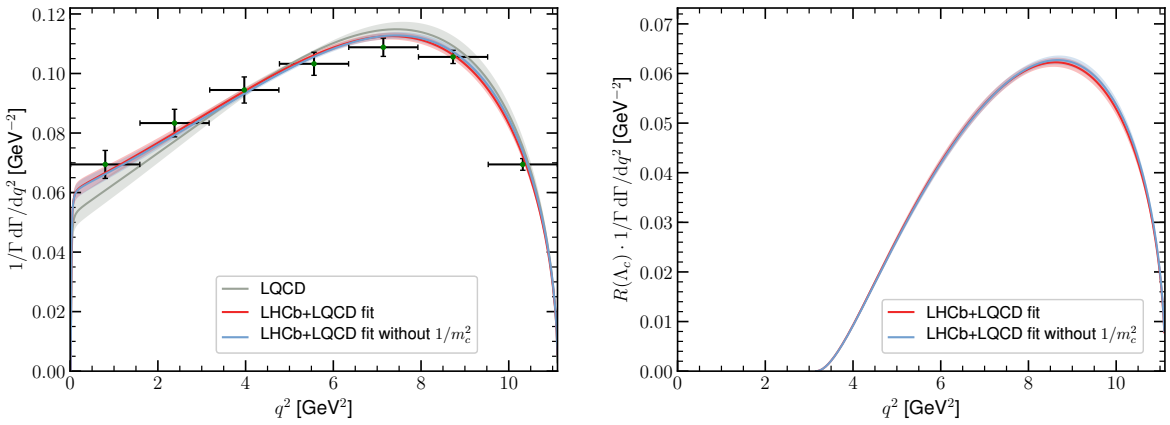

FIG. 1. Left: The data points show the LHCb measurement of the normalized $d\Gamma(\Lambda_b \to \Lambda_c \mu \bar{\nu})/dq^2$ spectrum [2]. The red band shows our fit of the HQET predictions to these data [2] and to the LQCD form factors [3]. The blue curve shows the fit results, setting the order $\Lambda^2_{\rm QCD}/m_c^2$ terms to zero. The gray band shows the LQCD prediction. Right: Our prediction for $d\Gamma(\Lambda_b \to \Lambda_c \tau \bar{\nu})/dq^2$ normalized to $R(\Lambda_c)$ from the same fit, with and without including the $\Lambda^2_{\rm QCD}/m_c^2$ terms.

III. FITS TO LHCb AND LATTICE QCD DATA

A. SM form factor fits

The methods used to fit $d\Gamma(\Lambda_b \to \Lambda_c \mu \bar{\nu})/dq^2$ measured by LHCb [2] and lattice QCD (LQCD) calculation of the (axial)vector form factors [3] were described in Ref. [1], and are only briefly recapitulated here. LHCb measured the q^2 spectrum in 7 bins, normalized to unity [2], reducing the effective degrees of freedom in the spectrum from 7 to 6. This measurement is shown as the data points in the left plot in Fig. 1. Our fits to the LHCb data use the measured and predicted partial rates in each bin. This procedure differs slightly from the fits performed by LHCb [2], which used the square root of $dN_{\rm corr}/dw$ evaluated at the midpoint in the seven unfolded w bins. The right plot in Fig. 1 shows our prediction for $1/\Gamma \times d\Gamma(\Lambda_b \to \Lambda_c \tau \bar{\nu})/dq^2$, normalized to $R(\Lambda_c)$.

The lattice QCD results [3] for the six (axial)vector form factors are published as fits to the BCL parametrization [54], using either 11 or 17 parameters. We derive predictions for $f_{1,2,3}$ and $g_{1,2,3}$ using the 17 parameter result at three q^2 values, $q^2 = \{1\,{\rm GeV}^2,\ q^2_{\rm max}/2,\ q^2_{\rm max} - 1\,{\rm GeV}^2\}$ for a total of eighteen form factor values, constructing a covariance matrix from their correlation structure. The values of q^2 are chosen to sample both ends and the middle of the

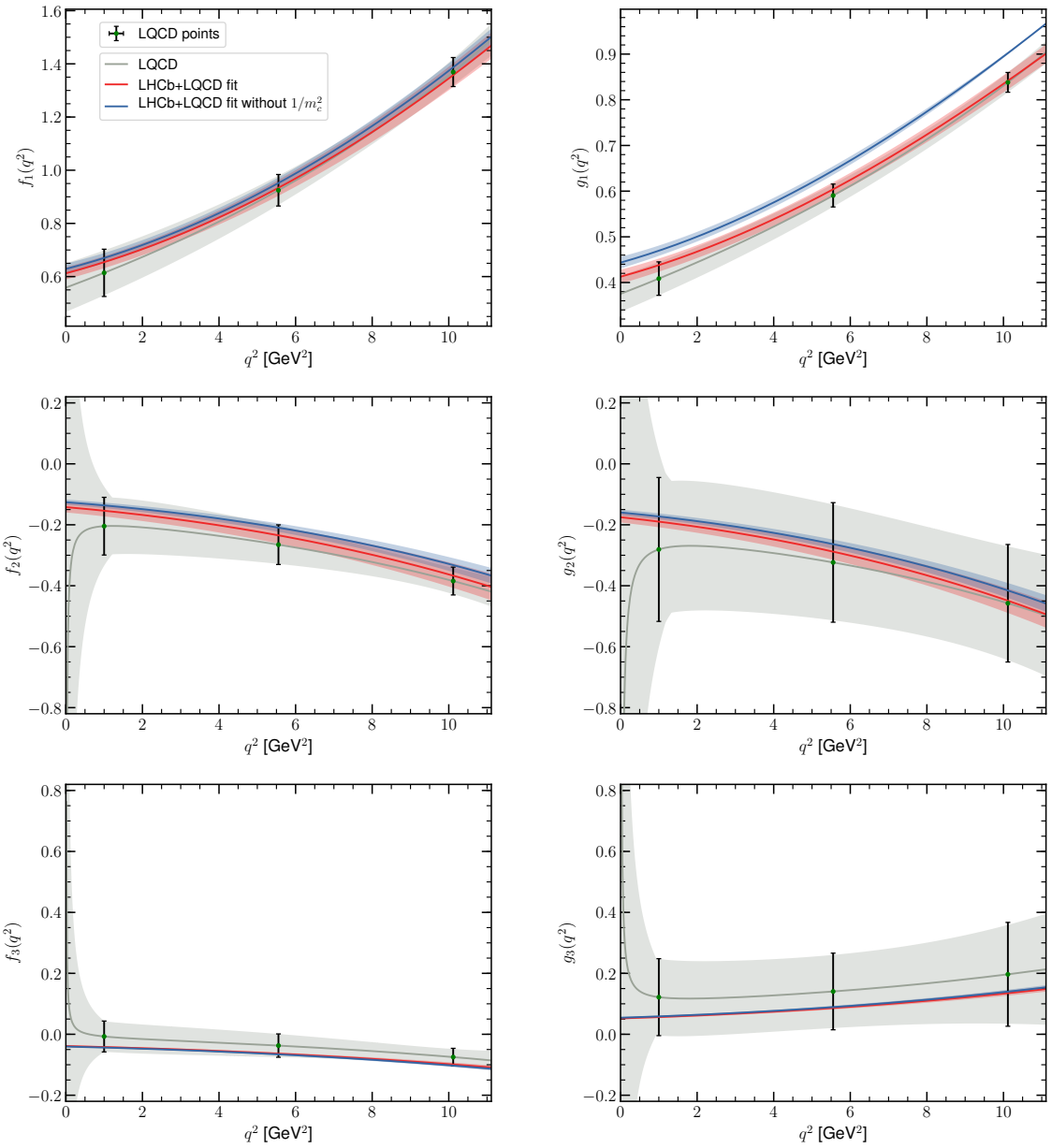

FIG. 2. Fits of the HQET predictions in Eq. (12) to the LQCD results [3] for the 6 form factors (red bands) for $f_{1,2,3}$ (left column) and $g_{1,2,3}$ (right column). The blue bands show the same fits, setting the order $\Lambda_{\rm QCD}^2/m_c^2$ terms to zero. Also shown are the LQCD predictions (gray bands and data points); see text for details.

q^2 spectrum. Adding more q^2 values from the BCL fit of the LQCD result to our sampling does not noticeably affect the fit results. The difference in the form factor values obtained using the 17 or the 11 BCL parameter results is added as an uncorrelated uncertainty. This slightly differs from the prescription in Ref. [3], which used the maximal differences of the

form factor values between the two parametrizations, and cannot preserve the correlation structure between the form factor values. The 18 form factor values used in our fits are shown as data points in Fig. 2. The LQCD predictions, following the prescription of Ref. [3], are shown as gray bands. The uncertainties are in good agreement. Similarly, the gray band in Fig. 1 (left plot) shows the LQCD prediction for the normalized spectrum, using the BCL parametrization.

In our fits, m_b^{1S} and δm_{bc} are constrained using Gaussian uncertainties. The leading order Isgur-Wise function is fitted to quadratic order in $w-1$

$$\zeta = 1 + (w-1)\,\zeta' + \frac{1}{2}(w-1)^2\,\zeta''\,. \tag{21}$$

Alternative expansions using the conformal parameters z or z^* [47, 54–56] instead of w yield nearly identical fits. Therefore, we do not explore the differences in the unitarity bounds between meson and baryon form factors [57]. Fits with ζ linear in either w, z, or z^* are poor, while adding more q^2 values to our sampling indicates no preference for the inclusion of higher order terms in $w-1$. In the fits $\hat{b}_{1,2}$ are assumed to be constants, which is appropriate at the current level of sensitivity. With better experimental and lattice constraints in the future, the sensitivity to lifting these assumptions should be tested.

Fit results combining the LHCb and LQCD results are shown in Table I, and in Fig. 2 by red bands. To test the importance of the $\Lambda_{\rm QCD}^2/m_c^2$ terms, we also perform a fit with the order $\Lambda_{\rm QCD}^2/m_c^2$ terms, parametrized by $\hat{b}_{1,2}$, set to zero. These fits are shown in Fig. 2 as blue bands, and the corresponding fit values are provided in Table I. This is a much poorer fit, changing χ^2/ndf from 7.2/20 to 18.8/22.

We do not include explicitly an uncertainty for neglected higher order terms in Eqs. (12) and (13). Four form factors, f_3, g_3, h_3, and h_4 receive no $\Lambda_{\rm QCD}^2/m_c^2$ corrections, so the agreement of f_3 and g_3 with the LQCD results in the plots in the bottom row in Fig. 2 indicates that these higher order corrections are probably small. The order $\varepsilon_c\,\varepsilon_b$ corrections to f_3 and g_3 are given by two new functions of w, b_5 and b_6 [27], while the ε_c^3 corrections to f_3 and g_3 also vanish. Thus, including such corrections, b_5 and b_6 would simply accommodate the $0.5\,\sigma - 1\,\sigma$ differences between the LQCD results and our fit for f_3 and g_3. The impact of this is small, for example, setting $f_3 = 0$ does not perceptibly change the SM prediction for $R(\Lambda_c)$ compared to Eq. (1), while setting $g_3 = 0$ changes the SM prediction from $R(\Lambda_c) = 0.324 \pm 0.004$ in Eq. 1 by about 1σ, to 0.320 ± 0.003.

	LHCb + LQCD	LHCb + LQCD
ζ'	-2.04 ± 0.08	-2.06 ± 0.08
ζ''	3.16 ± 0.38	3.28 ± 0.36
$\hat{b}_1/\text{GeV}^2$	-0.46 ± 0.15	0^*
$\hat{b}_2/\text{GeV}^2$	-0.39 ± 0.39	0^*
m_b^{1S}/GeV	4.72 ± 0.05	4.69 ± 0.04
$\delta m_{bc}/\text{GeV}$	3.40 ± 0.02	3.40 ± 0.02
χ^2/ndf	7.20/20	18.8/22
$R(\Lambda_c)$	0.3237 ± 0.0036	0.3252 ± 0.0035

TABLE I. HQET parameters extracted from the two fits discussed in the text. Predictions for $R(\Lambda_c)$ for each fit are shown in the last row. The $\hat{b}_{1,2}$ values marked with an asterisk were fixed to zero in the fit; see text for details.

In Fig. 3 show our fit results for ratios of form factors (red bands) and the LQCD predictions (gray bands). The top plot shows f_1/g_1, which HQET predicts to be $\mathcal{O}(1)$, whereas the four ratios f_2/f_1 and g_2/g_1 (second row) and f_3/f_1 and g_3/g_1 (third row) are predicted to be $\mathcal{O}(\varepsilon_{c,b},\, \alpha_s)$. The ratio, $f_1/g_1\,(= f_\perp/g_\perp)$, is determined by Eq. (12) as

$$\frac{f_1(w)}{g_1(w)} = 1 + \hat{\alpha}_s\left(C_{V_1} - C_{A_1}\right) + \left(\varepsilon_c + \varepsilon_b\right)\frac{2}{w+1} + \dots\,, \tag{22}$$

so the enhancement of f_1 relative to g_1 is a model independent prediction of HQET, as seen in the top plot in Fig. 3.

B. Tensor form factors

LQCD results [48] for the tensor form factors are available, and may be compared to HQET predictions from our fits to the (axial)vector form factors, via Eqs. (13).[2] The correspondence between the four form factors used in this paper for the tensor current, $\{h_1,\, h_2,\, h_3,\, h_4\}$, defined in Eq. (5), and those used in the LQCD calculation [48], $\{h_+,\, h_\perp,\, \widetilde{h}_+,\, \widetilde{h}_\perp\}$, are given in Appendix A. In the former basis, only one form factor, h_1, is nonzero in the heavy quark limit, while the four form factors of the LQCD basis are equal to one another in this limit. Note in particular that $h_1 = \widetilde{h}_+$.

[2] In Ref. [48] the equations of motions were used to express the scalar and pseudoscalar current matrix elements in terms of the axial and vector currents. The resulting expressions depend on the quark masses, $m_{b,c}$. It is inconsistent beyond leading order in α_s to use in such expressions the $\overline{\text{MS}}$ masses $\overline{m}_b(\overline{m}_b)$ and $\overline{m}_c(\overline{m}_c)$ [48] to evaluate the decay rates. Instead, one must use $\overline{m}_c(\mu)$ and $\overline{m}_b(\mu)$ at the same μ.

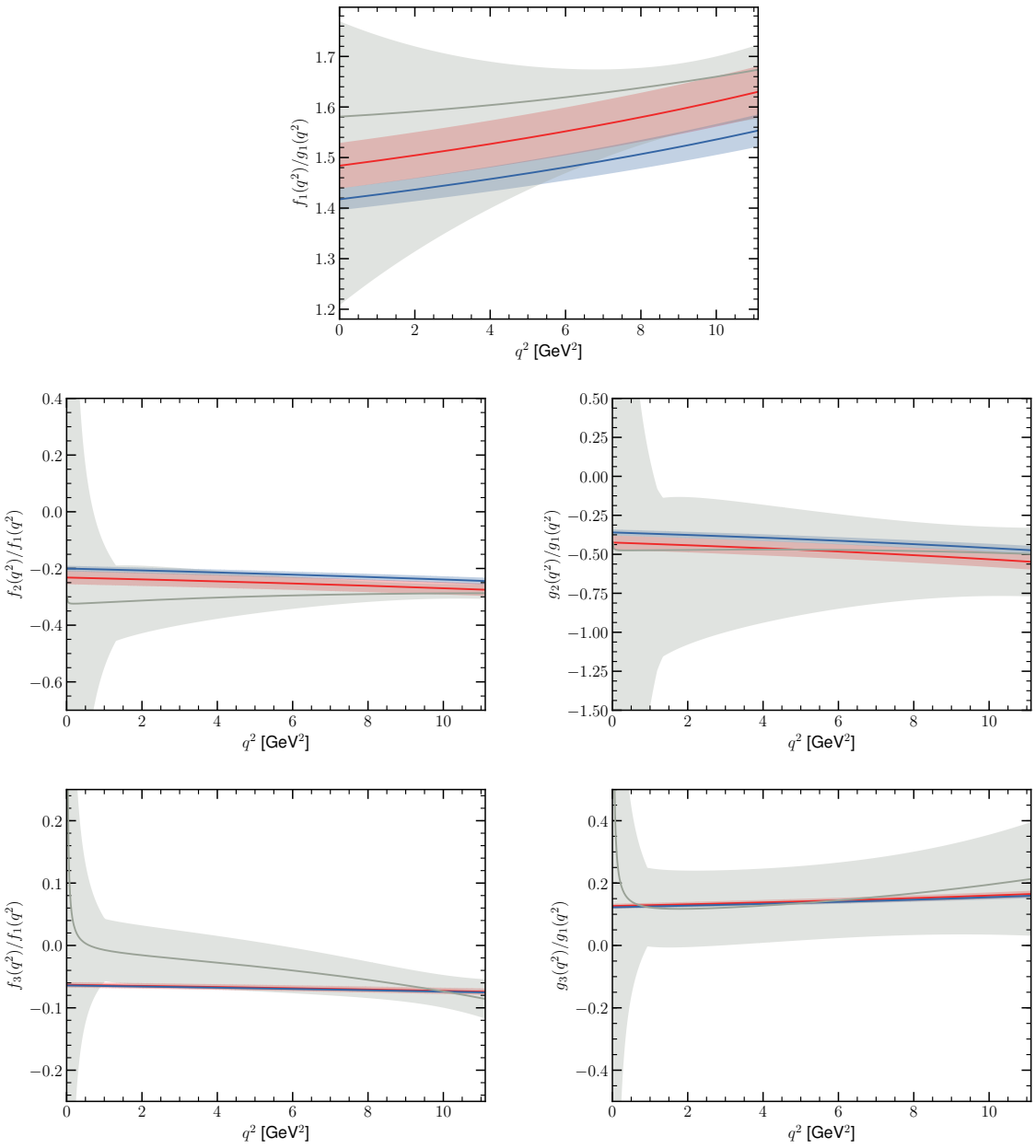

FIG. 3. Fits of the HQET predictions in Eq. (12) to the LQCD results [3], for five ratios of the six form factors. The top row shows f_1/g_1, which is $\mathcal{O}(1)$ in HQET, whereas $f_{2,3}/f_1$ (left column) and $g_{2,3}/g_1$ (right column) are expected to be $\mathcal{O}(\alpha_s, \Lambda_{\rm QCD}/m_Q)$. The red bands show our nominal fit including $\Lambda^2_{\rm QCD}/m_c^2$ terms; the blue bands show fit results with $\Lambda^2_{\rm QCD}/m_c^2$ terms set to zero.

The LQCD results [48] are presented using the BCL parametrization, including the correlations of the parameters. These results are computed at the scale $\mu = m_b$, while in this paper we match HQET onto QCD at $\mu = \sqrt{m_c m_b}$. Since the tensor current has a nonzero anoma-

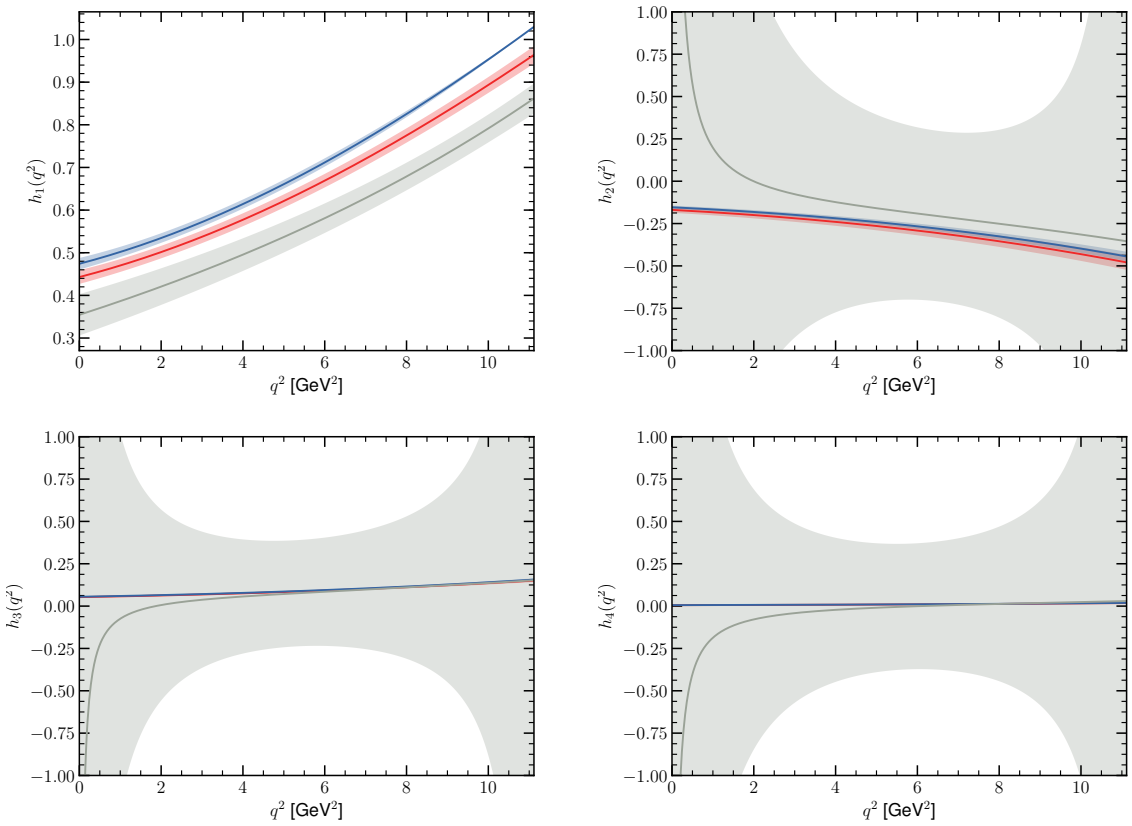

FIG. 4. Predictions for the tensor form factors based on Eq. (13) and our fit to the LHCb data and the LQCD calculation of the (axial)vector form factors, overlayed with the LQCD calculation of the tensor form factors [48] (scaled to $\mu = \sqrt{m_b m_c}$). The notation is the same as in Fig. 3.

lous dimension, we use the multiplicative renormalization factor $\left[\alpha_s(m_b)/\alpha_s(\sqrt{m_b m_c})\right]^{4/25} \simeq 0.97$ [58, 59], in order to scale the form factors to $\mu = \sqrt{m_b\, m_c}$.

In Fig. 4 the gray bands show the LQCD results for the tensor form factors converted to the $h_{1,2,3,4}$ basis. Our prediction from the fit to the (axial)vector SM form factors and the LHCb data are overlaid as red bands. The LQCD uncertainties are large for $h_{2,3,4}$ at both ends of the spectrum. This is an artifact of the $1/(w-1)$ and $1/q^2$ factors in the transformation from the LQCD basis in Eq. (A7). (The same information in the $\{h_+,\, h_\perp,\, \widetilde{h}_+,\, \widetilde{h}_\perp\}$ basis is shown in Fig. 7 in Appendix A. In this basis the uncertainties are not strongly q^2 dependent.) Unlike the fits in Sec. III A, the LQCD results for the tensor form factors are not an input to our fits, so there is no free parameter in these comparisons. Figure 7 shows that the order ε_c terms, which are fully determined by HQET in Eq. (13), combined with the definitions in Eq. (A6), account for the near equality of $\widetilde{h}_\perp$ and $\widetilde{h}_+$, the slight enhancement

of $h_\perp$, and the substantial enhancement of h_+. The top left plot in Fig. 4 shows a tension between our fit and the LQCD determination of $h_1 = \widetilde{h}_+$, visible in all plots in Fig. 7. In addition, the LQCD result for h_1 prefers a slightly smaller curvature than our prediction. This is similar to what is seen for f_1 and g_1 in the top row of Fig. 2: The LQCD results prefer a smaller curvature at small q^2. This is related to the observation that LQCD rate in Fig. 1 falls more quickly at small q^2 than the LHCb measurement.

C. $R(\Lambda_c)$ predictions with new physics

LHCb expects that the precision of the measurement of $R(\Lambda_c)$ can compete with that of $R(D^{(*)})$ in the future [60]. For the SM prediction we obtained [1]

$$R(\Lambda_c) = 0.324 \pm 0.004\,. \tag{23}$$

Our form factor fit, combined with the expressions for the NP rates in Appendix B and the HQET predictions in Eqs. (13), allows for precision computation of $R(\Lambda_c)$ for arbitrary NP contributions (see e.g. Refs [7, 9, 53] for prior analyses). To gain a sense of the sensitivity of $R(\Lambda_c)$, in Fig. 5, we show the allowed regions in the $R(\Lambda_c) - R(D)$ and $R(\Lambda_c) - R(D^*)$ planes, as any one of the five NP couplings in Eq. (3) are turned on. The boundary of each region corresponds to real NP Wilson coefficients, while the interior requires a relative phase between the SM and NP. The $V - A$ NP interaction cannot have a physical phase relative to the SM, and therefore spans a line in the $R(\Lambda_c) - R(D^{(*)})$ planes. Possibly by numerical coincidence, the scalar operator exhibits a very large correlation between $R(\Lambda_c)$ and $R(D)$, resulting in a very narrow $R(\Lambda_c) - R(D)$ region for this operator. Note that the (pseudo)scalar contributions vanish for the $D\,(D^*)$ modes, respectively, and are not shown.

In Fig. 6 we compare the variation in $R(\Lambda_c)/R(\Lambda_c)_{\rm SM}$ with the corresponding ratios for $D^{(*)}$, as a function of each NP coupling, assuming they are real. An error band, corresponding to the uncertainties in the fit of Ref. [1], is also shown. In some cases the errors are imperceptible. We see that the NP sensitivity of $R(\Lambda_c)$ is typically between the $R(D^*)$ and $R(D)$ variations.

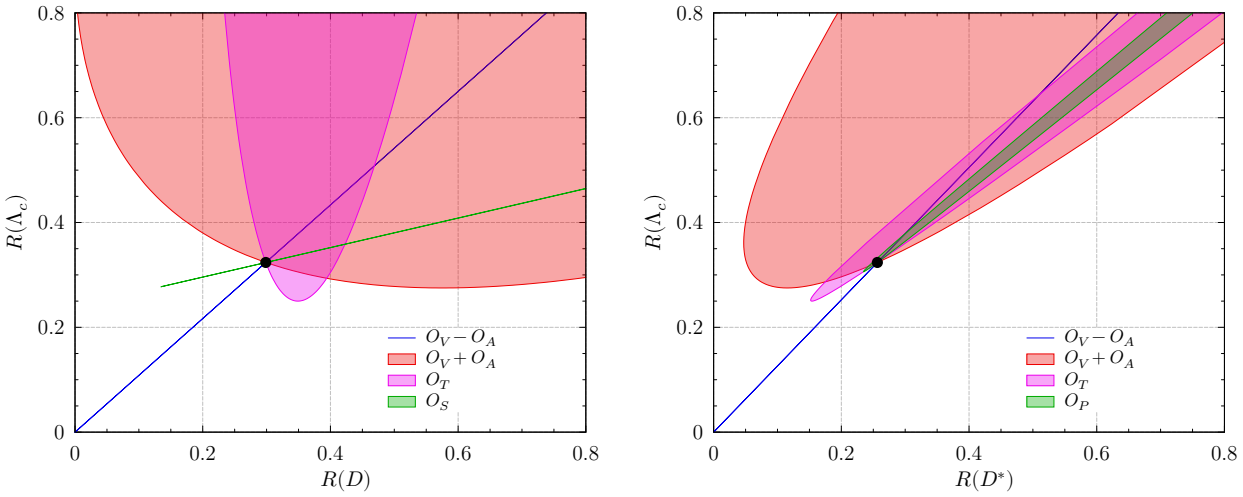

FIG. 5. $R(\Lambda_c)$ vs. $R(D)$ (left) and $R(D^*)$ (right) for various NP operators, in the basis defined in Eq. (3). The (pseudo)scalar contributions vanish for the $D(D^*)$ modes, and are not shown.

IV. FACTORIZATION AND $\Lambda_b \to \Lambda_c \pi$

The LHCb measurement of the $d\Gamma(\Lambda_b \to \Lambda_c^+ \mu^- \bar{\nu})/dq^2$ spectrum [2] is normalized to unity, and the LCQD results for the $\Lambda_b \to \Lambda_c$ form factors are also independent of $|V_{cb}|$. Thus, our fit is sensitive to hadronic parameters, but it cannot be combined with the present LHCb data to extract $|V_{cb}|$. One may, however, use the LHCb measurement of $d\Gamma(\Lambda_b \to \Lambda_c^+ \mu^- \bar{\nu})/dq^2$ to test factorization in $\Lambda_b \to \Lambda_c \pi$, or to extract $|V_{cb}|$ assuming factorization (see also Ref. [61]). For $B \to D^{(*)}\pi$ decays, it has long been known that the ratios $\mathcal{B}(B^- \to D^0 \pi^-)/\mathcal{B}(\bar{B}^0 \to D^+ \pi^-) \simeq 1.9$ and $\mathcal{B}(B^- \to D^{*0} \pi^-)/\mathcal{B}(\bar{B}^0 \to D^{*+} \pi^-) \simeq 1.8$ [29] deviate substantially from unity, the prediction in the heavy quark limit. This implies that $\mathcal{O}(\Lambda_{\rm QCD}/m_c)$ contributions to the amplitudes enter at the 30% level, and deviations from factorization in the heavy quark limit are substantial.

At leading order in the heavy quark expansion, the $\Lambda_b \to \Lambda_c \pi$ matrix element factorizes such that the nonleptonic rate is related to the semileptonic rate at $q^2 = m_\pi^2$ via

$$\Gamma(\Lambda_b \to \Lambda_c \pi) = 6\pi^2 \left(C_1 + C_2/3\right)^2 |V_{ud}|^2 f_\pi^2 \left.\frac{d\Gamma(\Lambda_b \to \Lambda_c e \bar{\nu})}{dq^2}\right|_{q^2 = m_\pi^2}, \tag{24}$$

where $f_\pi = 131\,\text{MeV}$ is the pion decay constant, and $C_{1,2}$ are the usual Wilson coefficients in the effective Hamiltonian, satisfying $(C_1 + C_2/3)\,|V_{ud}| \simeq 1$. (Uncertainties in this linear combination, f_π, and τ_{Λ_b} are neglected.) In Eq. (24), we write the $\Lambda_c e \bar{\nu}$ final state to emphasize that the semileptonic rate has to be evaluated neglecting lepton masses. In

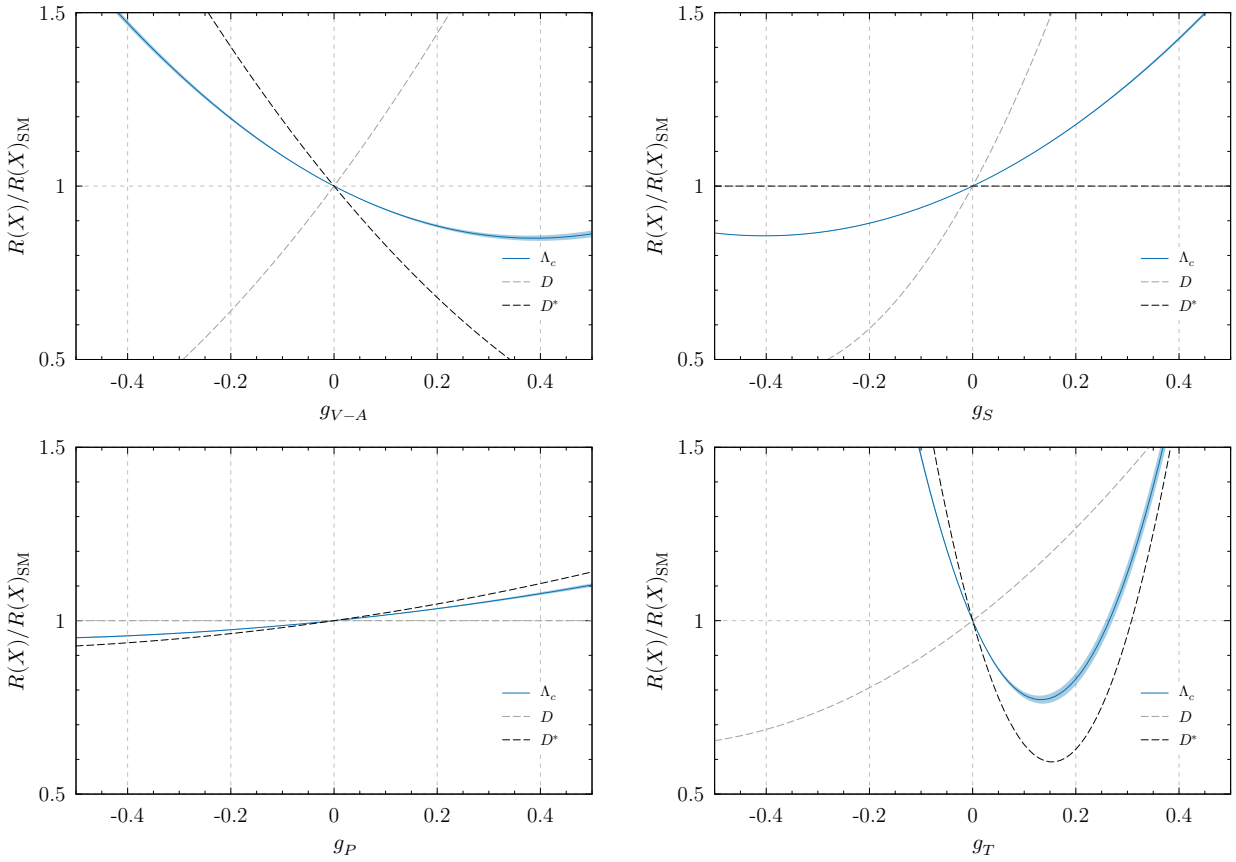

FIG. 6. $R(\Lambda_c)/R(\Lambda_c)_{\rm SM}$ and $R(D^{(*)})/R(D^{(*)})_{\rm SM}$ predictions for real NP couplings, in the operator basis of Eq. (3).

$\Lambda_b \to \Lambda_c \mu \bar{\nu}$ decay, measured by LHCb, the impact of $m_\mu \neq 0$ is substantial at $q^2 = m_\pi^2$.

Combining the factorization relation in Eq. (24), our fit for the form factors, and $|V_{cb}| = \big(4.22 \pm 0.08\big) \times 10^{-2}$ [29] predicts $\mathcal{B}(\Lambda_b \to \Lambda_c \pi) = (3.6 \pm 0.3) \times 10^{-3}$, where this uncertainty is from the fit and $|V_{cb}|$. By comparison, the measured nonleptonic branching ratio [29] is[3]

$$\mathcal{B}(\Lambda_b \to \Lambda_c \pi) = (4.9 \pm 0.5) \times 10^{-3} \,. \tag{25}$$

Conversely, assuming factorization, one could use Eqs. (25) in Eq. (24) to extract $|V_{cb}| = (4.9 \pm 0.3) \times 10^{-2}$, where this uncertainty is only from our form factor fit and the measured branching fraction, without an uncertainty assigned to the factorization relation itself. Thus

[3] This PDG average for $\mathcal{B}(\Lambda_b \to \Lambda_c \pi)$ includes an uncertainty scale factor of 1.5 [29], and is based on two LHCb [62, 63] and one CDF [64] measurements. Reproducing this is not easy, as it involves rescaling the CDF result from $\mathcal{B}(\Lambda_c \to p K^- \pi^+) = (5.0 \pm 1.3)\%$ to the latest values: $\mathcal{B}(\Lambda_c \to p K^- \pi^+) = (6.84 \pm 0.24^{+0.21}_{-0.27})\%$ [65] and $\mathcal{B}(\Lambda_c \to p K^- \pi^+) = (5.87 \pm 0.27 \pm 0.23)\%$ [66]. The LHCb measurements also preceded Ref. [66], and lifetime and other data also changed.

we observe an $\mathcal{O}(15\text{–}20\%)$ deviation from the factorization relation in Eq. (24), consistent with this deviation arising from a $\Lambda_{\rm QCD}/m_c$ suppressed correction [67]. [4]

V. CONCLUSIONS

Fitting the LHCb measurement of the normalized q^2 spectrum for $\Lambda_b \to \Lambda_c \mu\nu$ decay [2], and the six (axial)vector form factors calculated in lattice QCD [3], one can test HQET relations and the applicability of power counting. In Ref. [1] we found that the $\Lambda_{\rm QCD}^2/m_c^2$ corrections were constrained by the fit to be of the expected magnitude, without any signs of enhancements or breakdown of the power counting at the m_c scale, as is sometimes claimed in the literature. Compared to the lattice QCD only determination of the SM prediction of $R(\Lambda_c)$, by fitting the LHCb measurement as well, we further found that the uncertainty of the SM prediction may be substantially reduced, generating the most precise SM prediction for $R(\Lambda_c)$ to date, $R(\Lambda_c) = 0.324 \pm 0.004$.

We expanded and generalized the results of Ref. [1] in several ways. First, we calculated $\Lambda_b \to \Lambda_c$ semileptonic form factors for all four-Fermi NP operators, including the $\mathcal{O}(\Lambda_{\rm QCD}^2/m_c^2)$ corrections (as well as the corresponding helicity amplitudes for use in the `Hammer` library [71]). Using our fit of the LHCb measurement and the LQCD prediction for the six (axial)vector SM form factors, we obtained parameter-free predictions for the four tensor form factors at $\mathcal{O}(\Lambda_{\rm QCD}^2/m_c^2)$. We observed some tension between our results based on HQET and those in Ref. [48], at a magnitude greater than the $\Lambda_{\rm QCD}^2/m_c^2$ corrections (see the top left figure for the $h_1 = \widetilde{h}_+$ form factor in Fig. 4).

The small uncertainties in our fit to the (axial)vector form factors, combined with HQET predictions for the form factors at $\mathcal{O}(\Lambda_{\rm QCD}^2/m_c^2)$ allowed us to derive precise predictions for $R(\Lambda_c)$ for arbitrary NP. We studied the NP impacts on $R(\Lambda_c)$, including their correlations with $R(D^{(*)})$. The NP sensitivity of $R(\Lambda_c)$ typically falls between those of $R(D^*)$ and $R(D)$. We also explored tests of factorization in $\Lambda_b \to \Lambda_c \pi$ decay. Factorization in the heavy quark limit, combined with $|V_{cb}|$ measurements and our fit to the semileptonic form factors, implies a mildly lower nonleptonic rate than is measured, consistent with corrections to the factorization relations arising at $\mathcal{O}(\Lambda_{\rm QCD}/m_c)$.

[4] Regarding the behavior of the heavy quark expansion, the decay constants also satisfy the HQET scaling better than was thought in the 1990s. The $N_f = 2+1+1$ FLAG [68] averages, $f_B = (186 \pm 4)\,\text{MeV}$ and $f_D = (212 \pm 1.5)\,\text{MeV}$, yield $f_B/f_D \simeq 0.88$, which is not inconsistent with the leading order HQET relation [69, 70] $\sqrt{m_D/m_B}\,[\alpha_s(m_b)/\alpha_s(m_c)]^{-6/25} \simeq 0.68$, plus $\Lambda_{\rm QCD}/m_{c,b}$ corrections.

LHCb measurements of the double differential rate $d^2\Gamma(\Lambda_b \to \Lambda_c \ell \bar{\nu})/(dq^2\, d\cos\theta)$, in addition to the q^2 spectrum, will provide the most differential information measurable in the massless lepton channels (μ and e), if the details of the Λ_c decay are ignored. Besides the q^2 spectrum and the (q^2 dependent) forward-backward asymmetry, this double differential distribution involves a third function of q^2, which can help constrain form factors and test heavy quark symmetry. If the absolute normalization and the double differential rate of semileptonic $\Lambda_b \to \Lambda_c$ decays can be measured, it will provide a fully complementary path to extract $|V_{cb}|$, explore the $b \to c\tau\nu$ anomalies, and test HQET. We look forward to these developments.

ACKNOWLEDGMENTS

We thank Marina Artuso, Sheldon Stone, and Mark Wise for helpful conversations. We thank the Aspen Center of Physics, supported by the NSF grant PHY-1607611, where parts of this work were completed. FB and WS were supported by the DFG Emmy-Noether Grant No. BE 6075/1-1. ZL was supported in part by the U.S. Department of Energy under contract DE-AC02-05CH11231. The work of DR was supported in part by NSF grant PHY-1720252.

Appendix A: Form factor definitions, conversions, relations

The form factors in Eqs. (6) and (4) are related via [27]

$$
\begin{aligned}
F_1 &= f_1 + (m_{\Lambda_b} + m_{\Lambda_c})\left(\frac{f_2}{2m_{\Lambda_b}} + \frac{f_3}{2m_{\Lambda_c}}\right), \quad F_2 = -\frac{f_2}{2m_{\Lambda_b}} - \frac{f_3}{2m_{\Lambda_c}}, \quad F_3 = \frac{f_2}{2m_{\Lambda_b}} - \frac{f_3}{2m_{\Lambda_c}}, \\
G_1 &= g_1 - (m_{\Lambda_b} - m_{\Lambda_c})\left(\frac{g_2}{2m_{\Lambda_b}} + \frac{g_3}{2m_{\Lambda_c}}\right), \quad G_2 = -\frac{g_2}{2m_{\Lambda_b}} - \frac{g_3}{2m_{\Lambda_c}}, \quad G_3 = \frac{g_2}{2m_{\Lambda_b}} - \frac{g_3}{2m_{\Lambda_c}},
\end{aligned}
\tag{A1}
$$

or in the opposite direction,

$$
\begin{aligned}
f_1 &= F_1 + F_2\,(m_{\Lambda_b} + m_{\Lambda_c})\,, \qquad f_2 = (F_3 - F_2)\,m_{\Lambda_b}\,, \qquad f_3 = -(F_3 + F_2)\,m_{\Lambda_c}\,, \\
g_1 &= G_1 - G_2(m_{\Lambda_b} - m_{\Lambda_c})\,, \qquad g_2 = (G_3 - G_2)\,m_{\Lambda_b}\,, \qquad g_3 = -(G_3 + G_2)\,m_{\Lambda_c}\,.
\end{aligned}
\tag{A2}
$$

The form factors used in the lattice QCD calculation [3] and in the LHCb analysis [2]

follow the definitions in Ref. [72],

$$\begin{aligned}
\langle\Lambda_c(p',s')|\bar{q}\,\gamma_\mu\,b|\Lambda_b(p,s)\rangle &= \bar{u}(p',s')\left[f_0\,\frac{m_{\Lambda_b}-m_{\Lambda_c}}{q^2}\,q_\mu\right.\\
&\quad + f_+\,\frac{m_{\Lambda_b}+m_{\Lambda_c}}{s_+}\left(p_\mu+p'_\mu-\frac{m^2_{\Lambda_b}-m^2_{\Lambda_c}}{q^2}\,q_\mu\right)\\
&\quad \left.+ f_\perp\left(\gamma_\mu-\frac{2m_{\Lambda_c}}{s_+}\,p_\mu-\frac{2m_{\Lambda_b}}{s_+}\,p'_\mu\right)\right]u(p,s)\,,\\
\langle\Lambda_c(p',s')|\bar{q}\,\gamma_\mu\gamma_5\,b|\Lambda_b(p,s)\rangle &= -\bar{u}(p',s')\,\gamma_5\left[g_0\,\frac{m_{\Lambda_b}+m_{\Lambda_c}}{q^2}\,q_\mu\right.\\
&\quad + g_+\,\frac{m_{\Lambda_b}-m_{\Lambda_c}}{s_-}\left(p_\mu+p'_\mu-\frac{m^2_{\Lambda_b}-m^2_{\Lambda_c}}{q^2}\,q_\mu\right)\\
&\quad \left.+ g_\perp\left(\gamma_\mu+\frac{2m_{\Lambda_c}}{s_-}\,p_\mu-\frac{2m_{\Lambda_b}}{s_-}\,p'_\mu\right)\right]u(p,s)\,,
\end{aligned}\tag{A3}$$

where $q=p-p'$, and $s_\pm=(m_{\Lambda_b}\pm m_{\Lambda_c})^2-q^2=2\,m_{\Lambda_b}m_{\Lambda_c}(w\pm1)$. These form factors are related to the HQET form factors defined in Eq. (4) via

$$\begin{aligned}
f_1=f_\perp,\qquad f_2&=\frac{f_+-f_\perp}{w+1}-(f_+-f_0)\,\frac{1-r_\Lambda}{\hat{q}^2}\,,\\
f_3&=\frac{f_+-f_\perp}{w+1}+(f_+-f_0)\,\frac{r_\Lambda(1-r_\Lambda)}{\hat{q}^2}\,,\\
g_1=g_\perp,\qquad g_2&=\frac{g_+-g_\perp}{w-1}+(g_+-g_0)\,\frac{1+r_\Lambda}{\hat{q}^2}\,,\\
g_3&=\frac{g_+-g_\perp}{w-1}-(g_+-g_0)\,\frac{r_\Lambda(1+r_\Lambda)}{\hat{q}^2}\,.
\end{aligned}\tag{A4}$$

At $w=1$, corresponding to $q^2_{\rm max}$, the form factors satisfy $g_+(q^2_{\rm max})=g_\perp(q^2_{\rm max})$.

In the heavy quark limit, $f_0=f_+=f_\perp=g_0=g_+=g_\perp=\zeta+\mathcal{O}(\alpha_s,\,\Lambda_{\rm QCD}/m_{c,b})$. The lattice QCD results in Fig. 12 in Ref. [3] show that $f_0\,,\ f_+\,,\ g_0\,,\ g_+\,,\ g_\perp$ differ from one another by less than $\mathcal{O}(10\%)$, however, $f_\perp$ is substantially enhanced, consistent with the HQET prediction in Eq. (22).

The form factors in Eq. (A3), expressed in terms of the HQET definitions in Eq. (4), are

$$\begin{aligned}
f_\perp=f_1\,,\qquad f_0&=f_1+\frac{f_2(1-w\,r_\Lambda)+f_3(w-r_\Lambda)}{1-r_\Lambda}\,,\\
f_+&=f_1+(w+1)\,\frac{f_2\,r_\Lambda+f_3}{1+r_\Lambda}\,,\\
g_\perp=g_1\,,\qquad g_0&=g_1-\frac{g_2(1-w\,r_\Lambda)+g_3(w-r_\Lambda)}{1+r_\Lambda}\,,\\
g_+&=g_1-(w-1)\,\frac{g_2\,r_\Lambda+g_3}{1-r_\Lambda}\,.
\end{aligned}\tag{A5}$$

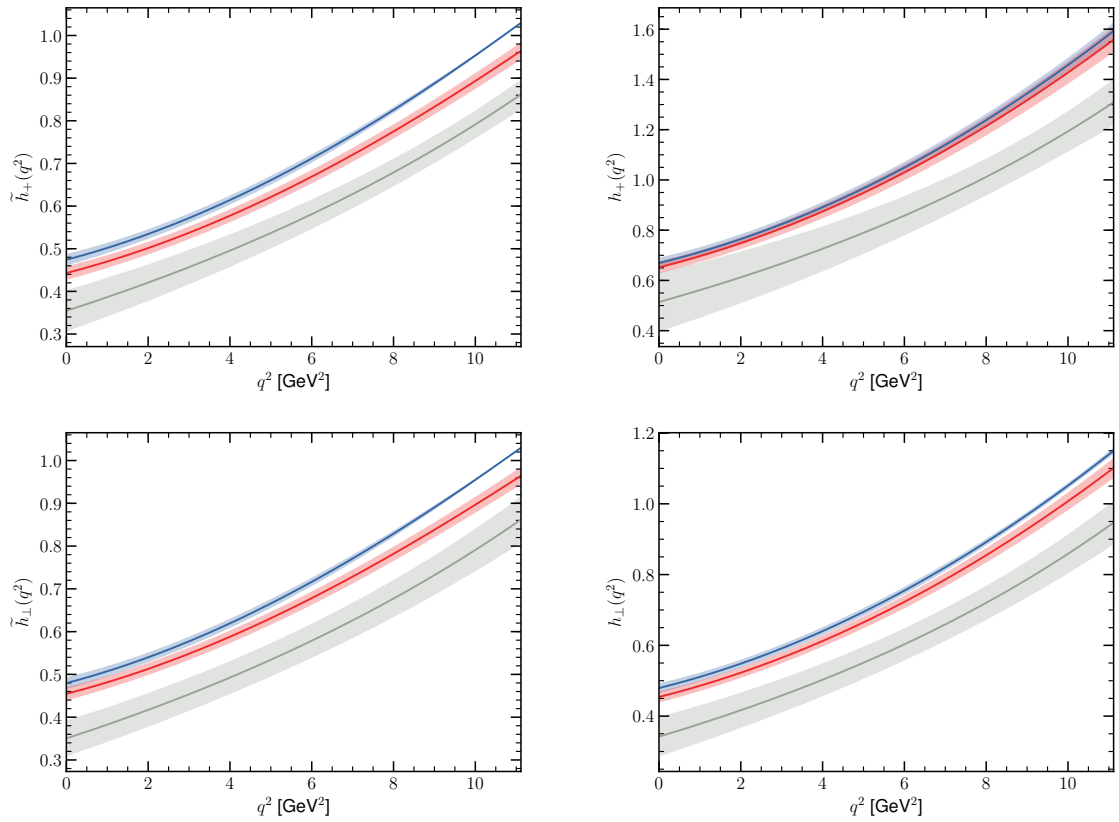

FIG. 7. Predictions for the tensor form factors in the basis used in the LQCD calculation [48] (scaled to $\mu = \sqrt{m_b m_c}$), compared with our predictions based on Eq. (13) and the fit to the LHCb data and the LQCD (axial)vector form factors. The notation is the same as in Fig. 4.

Finally, the translation between the $h_{1,2,3,4}$ tensor form factors used in this paper, defined in Eq. (5), and those defined in Eq. (2.14) in Ref. [48] are

$$\begin{aligned}
h_+ &= h_1 - h_2 + h_3 - h_4\,(w+1)\,,\\
h_\perp &= h_1 - h_2\,\frac{1 - w\,r_\Lambda}{1 + r_\Lambda} - h_3\,\frac{w - r_\Lambda}{1 + r_\Lambda}\,,\\
\widetilde{h}_+ &= h_1\,,\\
\widetilde{h}_\perp &= h_1 - \frac{h_2\,r_\Lambda + h_3}{1 - r_\Lambda}\,(w-1)\,,
\end{aligned} \tag{A6}$$

and in the opposite direction,

$$
\begin{aligned}
h_1 &= \widetilde{h}_+ \,, \\
h_2 &= \frac{\widetilde{h}_\perp - \widetilde{h}_+}{w-1} + \big(\widetilde{h}_\perp - h_\perp\big)\frac{1+r_\Lambda}{\hat{q}^2} \,, \\
h_3 &= \frac{\widetilde{h}_+ - \widetilde{h}_\perp}{w-1} + \big(h_\perp - \widetilde{h}_\perp\big)\frac{r_\Lambda(1+r_\Lambda)}{\hat{q}^2} \,, \\
h_4 &= \frac{\widetilde{h}_+ - \widetilde{h}_\perp}{w-1} + \frac{h_\perp - h_+}{w+1} + 2\big(h_\perp - \widetilde{h}_\perp\big)\frac{r_\Lambda}{\hat{q}^2} \,.
\end{aligned}
\tag{A7}
$$

In the heavy quark limit, the tensor form factors calculated in LQCD and shown in Fig. 2 of Ref. [48] satisfy $h_+ = h_\perp = \widetilde{h}_+ = \widetilde{h}_\perp = \zeta + \mathcal{O}(\alpha_s,\, \Lambda_{\rm QCD}/m_{c,b})$.

Appendix B: Amplitudes

In this appendix we collect explicit expressions for the $\Lambda_b \to \Lambda_c \ell \nu$ amplitudes, including mass terms and right-handed sterile neutrino contributions. These amplitudes correspond to those used in the `Hammer` code [71].

As in Ref. [73], we write explicit expressions for the $\bar{b} \to \bar{c}$ amplitudes rather than $b \to c$, defining the basis of NP operators to be

$$
\text{SM:} \quad i2\sqrt{2}\, V_{cb}^* G_F \big[\bar{b}\gamma^\mu P_L c\big]\big[\bar{\nu}\gamma_\mu P_L \ell\big] \,, \tag{B1a}
$$

$$
\text{Vector:} \quad i2\sqrt{2}\, V_{cb}^* G_F \big[\bar{b}\big(\alpha_L^V \gamma^\mu P_L + \alpha_R^V \gamma^\mu P_R\big)c\big]\big[\bar{\nu}\big(\beta_L^V \gamma_\mu P_L + \beta_R^V \gamma_\mu P_R\big)\ell\big] \,, \tag{B1b}
$$

$$
\text{Scalar:} \quad -i2\sqrt{2}\, V_{cb}^* G_F \big[\bar{b}\big(\alpha_L^S P_L + \alpha_R^S P_R\big)c\big]\big[\bar{\nu}\big(\beta_L^S P_R + \beta_R^S P_L\big)\ell\big] \,, \tag{B1c}
$$

$$
\text{Tensor:} \quad -i2\sqrt{2}\, V_{cb}^* G_F \big[\big(\bar{b}\alpha_R^T \sigma^{\mu\nu} P_R c\big)\big(\bar{\nu}\beta_L^T \sigma_{\mu\nu} P_R \ell\big) + \big(\bar{b}\alpha_L^T \sigma^{\mu\nu} P_L c\big)\big(\bar{\nu}\beta_R^T \sigma_{\mu\nu} P_L \ell\big)\big] \,. \tag{B1d}
$$

The lower index of β denotes the ν chirality and the lower index if α is that of the c quark. Operators for the CP conjugate $b \to c$ processes follow by Hermitian conjugation. (The correspondence between the α, β coefficients and the basis typically chosen for $b \to c$ operators can be found in Ref. [25].) The $\Lambda_b \to \Lambda_c \ell \nu$ process has four external spins: $s_b = \pm$, $s_c = 1, 2$, $s_\ell = 1, 2$ and $s_\nu = \pm$. (We label the Λ_c and ℓ spin by 1 and 2, to match the conventions of Ref. [73] for massive spinors on internal lines.)

Helicity angles and momenta are similarly defined with respect to the $\bar{b} \to \bar{c}$ process. Definitions for the conjugate process follow by replacing all particles with their antiparticles. The single physical polar helicity angle, θ_ℓ, defines the orientation of the lepton momenta in

their center of mass reference frame, with respect to $-\boldsymbol{p}_{\Lambda_b}$, as shown in Fig. 4 of Ref. [25]. Note that $\theta_\ell = \pi - \theta$, for θ defined in Eq. (14).

If subsequent $\Lambda_c \to \Lambda Y$ decays are included coherently, one further defines ϕ_ℓ and ϕ_Λ as twist angles of the ℓ–ν and Λ–Y decay planes, with the combination $\phi_\ell - \phi_\Lambda$ becoming a physical phase. Our phase conventions match the spinor conventions of Ref. [73] for not only τ but also Λ_c decay amplitudes. This amounts to requiring the inclusion in the τ and/or Λ_c decay amplitudes of an additional spinor phase function, $h_{s_\ell}(s_\nu)$ and $h_{s_c}(s_b)$, defined with respect to s_ν and s_b, such that $h_1(-) = 1 = h_2(+)$, $h_1(+) = e^{i\phi_\ell}$ and $h_2(-) = e^{-i\phi_\ell}$. Under these conventions, the $\Lambda_b \to \Lambda_c \ell\nu$ amplitudes themselves are independent of $\phi_\ell - \phi_\Lambda$.

For compact expression of the amplitudes, it is convenient to define

$$w_\pm = w \pm \sqrt{w^2-1}\,, \qquad \hat{q}^2 = q^2/m_{\Lambda_b}^2 = 1 - 2r_\Lambda w + r_\Lambda^2\,, \qquad r_\ell = m_\ell/m_{\Lambda_b}\,, \tag{B2}$$

along with

$$\begin{aligned}
\Sigma_+ &= \sqrt{w_+} + \sqrt{w_-}\,, & \Sigma_- &= \sqrt{w_+} - \sqrt{w_-}\,,\\
R_{+\pm} &= (1+r_\Lambda) \pm (1-r_\Lambda)\cos\theta_\ell\,, & R_{-\pm} &= (1-r_\Lambda) \pm (1+r_\Lambda)\cos\theta_\ell\,,\\
\Omega_+ &= r - w + \sqrt{w^2-1}\,\cos\theta_\ell\,, & \Omega_\times &= rw - 1 + r\sqrt{w^2-1}\,\cos\theta_\ell\,.
\end{aligned} \tag{B3}$$

The $\Lambda_b \to \Lambda_c \ell\nu$ amplitudes obey the conjugation relation

$$\mathcal{A}_{\bar{s}_b \bar{s}_c s_\ell s_\nu}\big(w, \sqrt{w^2-1}, \theta_\ell, \phi_\ell\big) = \mathcal{A}_{s_b s_c s_\ell s_\nu}\big(w, -\sqrt{w^2-1}, \pi - \theta_\ell, -\phi_\ell\big)\,, \tag{B4}$$

in which the exchange $\sqrt{w^2-1} \to -\sqrt{w^2-1}$ implies also $w_- \leftrightarrow w_+$. One then need only write the $s_b = -$ amplitudes, with the $s_b = +$ amplitudes following via Eq. (B4). Further writing $\mathcal{A} = 2\sqrt{2} G_F m_{\Lambda_b}^2 \sqrt{r_\Lambda(\hat{q}^2 - \rho_\ell)} \times A$, the explicit amplitudes are

$$\begin{aligned}
A_{-11-} = \Bigg\{ &- \frac{1}{2} h_S (\alpha_L^S + \alpha_R^S)\beta_L^S \Sigma_+ + \frac{1}{2} h_P (\alpha_L^S - \alpha_R^S)\beta_L^S \Sigma_-\\
&+ \frac{f_1 (1 + (\alpha_R^V + \alpha_L^V)\beta_L^V) r_\ell \big(\sqrt{w_-} R_{-+} + \sqrt{w_+} R_{--}\big)}{2\hat{q}^2}\\
&- \frac{f_3 (1 + (\alpha_R^V + \alpha_L^V)\beta_L^V) r_\ell \Sigma_+ \Omega_+}{2\hat{q}^2} - \frac{f_2 (1 + (\alpha_R^V + \alpha_L^V)\beta_L^V) r_\ell \Sigma_+ \Omega_\times}{2\hat{q}^2}\\
&+ \frac{g_1 (1 + (\alpha_L^V - \alpha_R^V)\beta_L^V) r_\ell \big(\sqrt{w_-} R_{++} - \sqrt{w_+} R_{+-}\big)}{2\hat{q}^2}\\
&- \frac{g_3 (1 + (\alpha_L^V - \alpha_R^V)\beta_L^V) r_\ell \Sigma_- \Omega_+}{2\hat{q}^2} - \frac{g_2 (1 + (\alpha_L^V - \alpha_R^V)\beta_L^V) r_\ell \Sigma_- \Omega_\times}{2\hat{q}^2}
\end{aligned}$$

$$
\begin{aligned}
&+ 4h_1\alpha_R^T\beta_L^T\sqrt{w_+}\cos\theta_\ell - 2h_2\alpha_R^T\beta_L^T\Sigma_-\cos\theta_\ell \\
&+ 2h_3\alpha_R^T\beta_L^T\Sigma_-\cos\theta_\ell - 2h_4\alpha_R^T\beta_L^T(w+1)\Sigma_-\cos\theta_\ell\Big\} \qquad \text{(B5a)}\\
A_{-11+} &= \sin\theta_\ell\Big\{\frac{(1+r_\Lambda)f_1(\alpha_L^V+\alpha_R^V)\beta_R^V\Sigma_-}{2\sqrt{\hat{q}^2}} \\
&+ \frac{r_\Lambda f_2(\alpha_L^V+\alpha_R^V)\beta_R^V(w+1)\Sigma_-}{2\sqrt{\hat{q}^2}} + \frac{f_3(\alpha_L^V+\alpha_R^V)\beta_R^V(w+1)\Sigma_-}{2\sqrt{\hat{q}^2}} \\
&+ \frac{(r_\Lambda-1)g_1(\alpha_L^V-\alpha_R^V)\beta_R^V\Sigma_+}{2\sqrt{\hat{q}^2}} \\
&+ \frac{r_\Lambda g_2(\alpha_L^V-\alpha_R^V)\beta_R^V(w-1)\Sigma_+}{2\sqrt{\hat{q}^2}} + \frac{g_3(\alpha_L^V-\alpha_R^V)\beta_R^V(w-1)\Sigma_+}{2\sqrt{\hat{q}^2}} \\
&+ 4h_1\alpha_L^T\beta_R^T r_\ell\sqrt{\frac{w_-}{\hat{q}^2}} + \frac{2h_2\alpha_L^T\beta_R^T r_\ell\Sigma_-}{\sqrt{\hat{q}^2}} \\
&- \frac{2h_3\alpha_L^T\beta_R^T r_\ell\Sigma_-}{\sqrt{\hat{q}^2}} + \frac{2h_4\alpha_L^T\beta_R^T r_\ell(w+1)\Sigma_-}{\sqrt{\hat{q}^2}}\Big\} \qquad \text{(B5b)}\\
A_{-12-} &= \sin\theta_\ell\Big\{\frac{(1+r_\Lambda)f_1(1+(\alpha_R^V+\alpha_L^V)\beta_L^V)\Sigma_-}{2\sqrt{\hat{q}^2}} \\
&+ \frac{r_\Lambda f_2(1+(\alpha_R^V+\alpha_L^V)\beta_L^V)(w+1)\Sigma_-}{2\sqrt{\hat{q}^2}} + \frac{f_3(1+(\alpha_R^V+\alpha_L^V)\beta_L^V)(w+1)\Sigma_-}{2\sqrt{\hat{q}^2}} \\
&+ \frac{(r_\Lambda-1)g_1(1+(\alpha_L^V-\alpha_R^V)\beta_L^V)\Sigma_+}{2\sqrt{\hat{q}^2}} \\
&+ \frac{r_\Lambda g_2(1+(\alpha_L^V-\alpha_R^V)\beta_L^V)(w-1)\Sigma_+}{2\sqrt{\hat{q}^2}} + \frac{g_3(1+(\alpha_L^V-\alpha_R^V)\beta_L^V)(w-1)\Sigma_+}{2\sqrt{\hat{q}^2}} \\
&- 4h_1\alpha_R^T\beta_L^T r_\ell\sqrt{\frac{w_+}{\hat{q}^2}} + \frac{2h_2\alpha_R^T\beta_L^T r_\ell\Sigma_-}{\sqrt{\hat{q}^2}} \\
&- \frac{2h_3\alpha_R^T\beta_L^T r_\ell\Sigma_-}{\sqrt{\hat{q}^2}} + \frac{2h_4\alpha_R^T\beta_L^T r_\ell(w+1)\Sigma_-}{\sqrt{\hat{q}^2}}\Big\} \qquad \text{(B5c)}\\
A_{-12+} &= \Big\{\frac{1}{2}h_S(\alpha_L^S+\alpha_R^S)\beta_R^S\Sigma_+ - \frac{1}{2}h_P(\alpha_L^S-\alpha_R^S)\beta_R^S\Sigma_- \\
&- \frac{f_1(\alpha_L^V+\alpha_R^V)\beta_R^V r_\ell\big(\sqrt{w_-}R_{-+}+\sqrt{w_+}R_{--}\big)}{2\hat{q}^2} \\
&+ \frac{f_3(\alpha_L^V+\alpha_R^V)\beta_R^V r_\ell\Sigma_+\Omega_+}{2\hat{q}^2} + \frac{f_2(\alpha_L^V+\alpha_R^V)\beta_R^V r_\ell\Sigma_+\Omega_\times}{2\hat{q}^2} \\
&- \frac{g_1(\alpha_L^V-\alpha_R^V)\beta_R^V r_\ell\big(\sqrt{w_-}R_{++}-\sqrt{w_+}R_{+-}\big)}{2\hat{q}^2} \\
&+ \frac{g_3(\alpha_L^V-\alpha_R^V)\beta_R^V r_\ell\Sigma_-\Omega_+}{2\hat{q}^2} + \frac{g_2(\alpha_L^V-\alpha_R^V)\beta_R^V r_\ell\Sigma_-\Omega_\times}{2\hat{q}^2}
\end{aligned}
$$

$$
\begin{aligned}
&+ 4h_1\alpha_L^T\beta_R^T\sqrt{w_-}\cos\theta_\ell + 2h_2\alpha_L^T\beta_R^T\Sigma_-\cos\theta_\ell \\
&- 2h_3\alpha_L^T\beta_R^T\Sigma_-\cos\theta_\ell + 2h_4\alpha_L^T\beta_R^T(w+1)\Sigma_-\cos\theta_\ell\Big\} \qquad \text{(B5d)}\\
A_{-21-} &= \sin\theta_\ell\Big\{\frac{f_1(1+(\alpha_R^V+\alpha_L^V)\beta_L^V)r_\ell\Sigma_-}{2\sqrt{\hat{q}^2}} \\
&+ \frac{g_1(1+(\alpha_L^V-\alpha_R^V)\beta_L^V)r_\ell\Sigma_+}{2\sqrt{\hat{q}^2}} \\
&+ \frac{4h_1\alpha_R^T\beta_L^T(w_- - r_\Lambda)}{\sqrt{\hat{q}^2 w_-}} - \frac{2h_2\alpha_R^T\beta_L^T(r_\Lambda w_+ - 1)\Sigma_-}{\sqrt{\hat{q}^2}} \\
&- \frac{2h_3\alpha_R^T\beta_L^T(r_\Lambda - w_-)\Sigma_-}{\sqrt{\hat{q}^2}}\Big\} \qquad \text{(B5e)}\\
A_{-21+} &= \sin^2\frac{\theta_\ell}{2}\Big\{ - f_1(\alpha_L^V+\alpha_R^V)\beta_R^V\Sigma_- \\
&+ g_1(-\alpha_L^V+\alpha_R^V)\beta_R^V\Sigma_+ \\
&- \frac{8h_1\alpha_L^T\beta_R^T r_\ell\sqrt{w_+}(r_\Lambda w_- - 1)}{\hat{q}^2} + \frac{4h_2\alpha_L^T\beta_R^T r_\ell(r_\Lambda w_- - 1)\Sigma_-}{\hat{q}^2} \\
&- \frac{4h_3\alpha_L^T\beta_R^T r_\ell(w_+ - r_\Lambda)\Sigma_-}{\hat{q}^2}\Big\} \qquad \text{(B5f)}\\
A_{-22-} &= \cos^2\frac{\theta_\ell}{2}\Big\{f_1(1+(\alpha_R^V+\alpha_L^V)\beta_L^V)\Sigma_- \\
&+ g_1(1+(\alpha_L^V-\alpha_R^V)\beta_L^V)\Sigma_+ \\
&- \frac{8h_1\alpha_R^T\beta_L^T r_\ell(r_\Lambda w_+ - 1)\sqrt{w_-}}{\hat{q}^2} - \frac{4h_2\alpha_R^T\beta_L^T r_\ell(r_\Lambda w_+ - 1)\Sigma_-}{\hat{q}^2} \\
&- \frac{4h_3\alpha_R^T\beta_L^T r_\ell(r_\Lambda - w_-)\Sigma_-}{\hat{q}^2}\Big\} \qquad \text{(B5g)}\\
A_{-22+} &= \sin\theta_\ell\Big\{ - \frac{f_1(\alpha_L^V+\alpha_R^V)\beta_R^V r_\ell\Sigma_-}{2\sqrt{\hat{q}^2}} \\
&+ \frac{g_1(-\alpha_L^V+\alpha_R^V)\beta_R^V r_\ell\Sigma_+}{2\sqrt{\hat{q}^2}} \\
&+ \frac{4h_1\alpha_L^T\beta_R^T(w_+ - r_\Lambda)}{\sqrt{\hat{q}^2 w_+}} + \frac{2h_2\alpha_L^T\beta_R^T(r_\Lambda w_- - 1)\Sigma_-}{\sqrt{\hat{q}^2}} \\
&- \frac{2h_3\alpha_L^T\beta_R^T(w_+ - r_\Lambda)\Sigma_-}{\sqrt{\hat{q}^2}}\Big\}. \qquad \text{(B5h)}
\end{aligned}
$$

The total differential rate for $\Lambda_b \to \Lambda_c\ell\nu$ is obtained from these expressions via

$$
d\Gamma = \frac{G_F^2 m_{\Lambda_b}^5 r_\Lambda^3 |V_{cb}|^2}{32\pi^3}\sqrt{w^2-1}\frac{(\hat{q}^2-\rho_\ell)^2}{\hat{q}^2}\sum_{s_b,s_c,s_\ell,s_\nu}|A_{s_b,s_c,s_\ell,s_\nu}|^2 dw\,\sin\theta_\ell d\theta_\ell\,. \qquad \text{(B6)}
$$

[1] F. U. Bernlochner, Z. Ligeti, D. J. Robinson, and W. L. Sutcliffe, Phys. Rev. Lett. **121**, 202001 (2018), arXiv:1808.09464 [hep-ph].

[2] R. Aaij *et al.* (LHCb Collaboration), Phys. Rev. **D96**, 112005 (2017), arXiv:1709.01920 [hep-ex].

[3] W. Detmold, C. Lehner, and S. Meinel, Phys. Rev. **D92**, 034503 (2015), arXiv:1503.01421 [hep-lat].

[4] H. Georgi, Phys. Lett. **B240**, 447 (1990).

[5] E. Eichten and B. R. Hill, Phys. Lett. **B234**, 511 (1990).

[6] R. M. Woloshyn, *Proceedings, 15th International Conference on Hadron Spectroscopy (Hadron 2013): Nara, Japan, November 4-8, 2013*, PoS **Hadron2013**, 203 (2013).

[7] S. Shivashankara, W. Wu, and A. Datta, Phys. Rev. **D91**, 115003 (2015), arXiv:1502.07230 [hep-ph].

[8] T. Gutsche, M. A. Ivanov, J. G. Korner, V. E. Lyubovitskij, P. Santorelli, and N. Habyl, Phys. Rev. **D91**, 074001 (2015), [Erratum: Phys. Rev.D91,no.11,119907(2015)], arXiv:1502.04864 [hep-ph].

[9] R. Dutta, Phys. Rev. **D93**, 054003 (2016), arXiv:1512.04034 [hep-ph].

[10] Phys. Rev. **D97**, 074007 (2018), arXiv:1803.02085 [hep-ph].

[11] E. Di Salvo, F. Fontanelli, and Z. J. Ajaltouni, Int. J. Mod. Phys. **A33**, 1850169 (2018), arXiv:1804.05592 [hep-ph].

[12] Y. Amhis *et al.* (Heavy Flavor Averaging Group), Eur. Phys. J. **C77**, 895 (2017), and updates at `http://www.slac.stanford.edu/xorg/hfag/`, arXiv:1612.07233 [hep-ex].

[13] F. U. Bernlochner, Z. Ligeti, M. Papucci, and D. J. Robinson, Phys. Rev. **D95**, 115008 (2017), arXiv:1703.05330 [hep-ph].

[14] D. Bigi, P. Gambino, and S. Schacht, JHEP **11**, 061 (2017), arXiv:1707.09509 [hep-ph].

[15] S. Jaiswal, S. Nandi, and S. K. Patra, JHEP **12**, 060 (2017), arXiv:1707.09977 [hep-ph].

[16] D. Bigi, P. Gambino, and S. Schacht, Phys. Lett. **B769**, 441 (2017), arXiv:1703.06124 [hep-ph].

[17] B. Grinstein and A. Kobach, Phys. Lett. **B771**, 359 (2017), arXiv:1703.08170 [hep-ph].

[18] F. U. Bernlochner, Z. Ligeti, M. Papucci, and D. J. Robinson, Phys. Rev. **D96**, 091503

(2017), arXiv:1708.07134 [hep-ph].

[19] J. A. Bailey *et al.* (Fermilab Lattice and MILC Collaborations), Phys. Rev. **D92**, 034506 (2015), arXiv:1503.07237 [hep-lat].

[20] *Proceedings, 35th International Symposium on Lattice Field Theory (Lattice 2017): Granada, Spain, June 18-24, 2017*, EPJ Web Conf. **175**, 13003 (2018), arXiv:1710.09817 [hep-lat].

[21] T. Kaneko, Y. Aoki, B. Colquhoun, H. Fukaya, and S. Hashimoto (JLQCD) (2018) arXiv:1811.00794 [hep-lat].

[22] A. K. Leibovich, Z. Ligeti, I. W. Stewart, and M. B. Wise, Phys. Rev. Lett. **78**, 3995 (1997), arXiv:hep-ph/9703213 [hep-ph].

[23] A. K. Leibovich, Z. Ligeti, I. W. Stewart, and M. B. Wise, Phys. Rev. **D57**, 308 (1998), arXiv:hep-ph/9705467 [hep-ph].

[24] F. U. Bernlochner and Z. Ligeti, Phys. Rev. **D95**, 014022 (2017), arXiv:1606.09300 [hep-ph].

[25] F. U. Bernlochner, Z. Ligeti, and D. J. Robinson, Phys. Rev. **D97**, 075011 (2018), arXiv:1711.03110 [hep-ph].

[26] N. Isgur and M. B. Wise, Nucl. Phys. **B348**, 276 (1991).

[27] A. F. Falk and M. Neubert, Phys. Rev. **D47**, 2982 (1993), arXiv:hep-ph/9209269 [hep-ph].

[28] A. V. Manohar and M. B. Wise, Camb. Monogr. Part. Phys. Nucl. Phys. Cosmol. **10**, 1 (2000).

[29] M. Tanabashi *et al.* (Particle Data Group), Phys. Rev. **D98**, 030001 (2018).

[30] A. H. Hoang, Z. Ligeti, and A. V. Manohar, Phys. Rev. Lett. **82**, 277 (1999), arXiv:hep-ph/9809423 [hep-ph].

[31] A. H. Hoang, Z. Ligeti, and A. V. Manohar, Phys. Rev. **D59**, 074017 (1999), arXiv:hep-ph/9811239 [hep-ph].

[32] A. H. Hoang, Phys. Rev. **D61**, 034005 (2000), arXiv:hep-ph/9905550 [hep-ph].

[33] Z. Ligeti and F. J. Tackmann, Phys. Rev. **D90**, 034021 (2014), arXiv:1406.7013 [hep-ph].

[34] C. W. Bauer, Z. Ligeti, M. Luke, A. V. Manohar, and M. Trott, Phys. Rev. **D70**, 094017 (2004), arXiv:hep-ph/0408002 [hep-ph].

[35] C. W. Bauer, Z. Ligeti, M. Luke, and A. V. Manohar, Phys. Rev. **D67**, 054012 (2003), arXiv:hep-ph/0210027 [hep-ph].

[36] A. K. Leibovich and I. W. Stewart, Phys. Rev. **D57**, 5620 (1998), arXiv:hep-ph/9711257 [hep-ph].

[37] P. Boer, M. Bordone, E. Graverini, P. Owen, M. Rotondo, and D. Van Dyk, JHEP **06**, 155

(2018), arXiv:1801.08367 [hep-ph].

[38] A. F. Falk, H. Georgi, B. Grinstein, and M. B. Wise, Nucl. Phys. **B343**, 1 (1990).

[39] A. F. Falk and B. Grinstein, Phys. Lett. **B249**, 314 (1990).

[40] M. Neubert, Nucl. Phys. **B371**, 149 (1992).

[41] H. Georgi, B. Grinstein, and M. B. Wise, Phys. Lett. **B252**, 456 (1990).

[42] M. E. Luke, Phys. Lett. **B252**, 447 (1990).

[43] M. Neubert, Phys. Lett. **B306**, 357 (1993), arXiv:hep-ph/9302269 [hep-ph].

[44] M. Neubert, Phys. Rept. **245**, 259 (1994), arXiv:hep-ph/9306320 [hep-ph].

[45] P. Asadi, M. R. Buckley, and D. Shih, JHEP **09**, 010 (2018), arXiv:1804.04135 [hep-ph].

[46] A. Greljo, D. J. Robinson, B. Shakya, and J. Zupan, JHEP **09**, 169 (2018), arXiv:1804.04642 [hep-ph].

[47] C. G. Boyd, B. Grinstein, and R. F. Lebed, Phys. Rev. **D56**, 6895 (1997), arXiv:hep-ph/9705252 [hep-ph].

[48] A. Datta, S. Kamali, S. Meinel, and A. Rashed, JHEP **08**, 131 (2017), arXiv:1702.02243 [hep-ph].

[49] K. S. M. Lee, Z. Ligeti, I. W. Stewart, and F. J. Tackmann, Phys. Rev. **D75**, 034016 (2007), arXiv:hep-ph/0612156 [hep-ph].

[50] J. G. Korner and M. Kramer, Phys. Lett. **B275**, 495 (1992), (Note that a sign mistake is corrected in Ref. [52]).

[51] G. D. Crawford *et al.* (CLEO Collaboration), Phys. Rev. Lett. **75**, 624 (1995).

[52] J. W. Hinson *et al.* (CLEO Collaboration), Phys. Rev. Lett. **94**, 191801 (2005), arXiv:hep-ex/0501002 [hep-ex].

[53] X.-Q. Li, Y.-D. Yang, and X. Zhang, JHEP **02**, 068 (2017), arXiv:1611.01635 [hep-ph].

[54] C. Bourrely, I. Caprini, and L. Lellouch, Phys. Rev. **D79**, 013008 (2009), [Erratum: Phys. Rev. D82, 099902 (2010)], arXiv:0807.2722 [hep-ph].

[55] C. G. Boyd, B. Grinstein, and R. F. Lebed, Nucl. Phys. **B461**, 493 (1996), arXiv:hep-ph/9508211 [hep-ph].

[56] C. G. Boyd and M. J. Savage, Phys. Rev. **D56**, 303 (1997), arXiv:hep-ph/9702300 [hep-ph].

[57] C. G. Boyd and R. F. Lebed, Nucl. Phys. **B485**, 275 (1997), arXiv:hep-ph/9512363 [hep-ph].

[58] I. Dorsner, S. Fajfer, N. Kosnik, and I. Nisandzic, JHEP **11**, 084 (2013), arXiv:1306.6493 [hep-ph].

[59] M. Freytsis, Z. Ligeti, and J. T. Ruderman, Phys. Rev. **D92**, 054018 (2015), arXiv:1506.08896 [hep-ph].

[60] P. Alvarez Cartelle (LHCb Collaboration), Talk at the Workshop on the physics of HL-LHC, and perspectives at HE-LHC (2017), `https://indico.cern.ch/event/647676/contributions/2758167/attachments/1549660/2434073/RareDecays_HLLHC.pdf`.

[61] A. K. Leibovich, Z. Ligeti, I. W. Stewart, and M. B. Wise, Phys. Lett. **B586**, 337 (2004), arXiv:hep-ph/0312319 [hep-ph].

[62] R. Aaij *et al.* (LHCb Collaboration), JHEP **04**, 087 (2014), arXiv:1402.0770 [hep-ex].

[63] R. Aaij *et al.* (LHCb Collaboration), JHEP **08**, 143 (2014), arXiv:1405.6842 [hep-ex].

[64] A. Abulencia *et al.* (CDF Collaboration), Phys. Rev. Lett. **98**, 122002 (2007), arXiv:hep-ex/0601003 [hep-ex].

[65] A. Zupanc *et al.* (Belle Collaboration), Phys. Rev. Lett. **113**, 042002 (2014), arXiv:1312.7826 [hep-ex].

[66] M. Ablikim *et al.* (BESIII Collaboration), Phys. Rev. Lett. **116**, 052001 (2016), arXiv:1511.08380 [hep-ex].

[67] C. W. Bauer, D. Pirjol, and I. W. Stewart, Phys. Rev. Lett. **87**, 201806 (2001), arXiv:hep-ph/0107002 [hep-ph].

[68] S. Aoki *et al.*, Eur. Phys. J. **C77**, 112 (2017), arXiv:1607.00299 [hep-lat], and updates at `http://flag.unibe.ch/`.

[69] H. D. Politzer and M. B. Wise, Phys. Lett. **B206**, 681 (1988).

[70] M. A. Shifman and M. B. Voloshin, Sov. J. Nucl. Phys. **45**, 292 (1987), [Yad. Fiz. **45**, 463 (1987)].

[71] S. Duell, F. Bernlochner, Z. Ligeti, M. Papucci, and D. Robinson, *Proceedings, 38th International Conference on High Energy Physics (ICHEP 2016): Chicago, IL, USA, August 3-10, 2016*, PoS **ICHEP2016**, 1074 (2017).

[72] T. Feldmann and M. W. Y. Yip, Phys. Rev. **D85**, 014035 (2012), [Erratum: Phys. Rev.D86,079901(2012)], arXiv:1111.1844 [hep-ph].

[73] Z. Ligeti, M. Papucci, and D. J. Robinson, JHEP **01**, 083 (2017), arXiv:1610.02045 [hep-ph].